

B. M. Sabirov

**MUONS and NUCLEI,**  
or  
**The Adventures of the Muon  
in the Nucleus**

Joint Institute for Nuclear Research

B. M. Sabirov

MUONS AND NUCLEI,  
or  
The Adventures of the Muon  
in the Nucleus

Dubna 2024

УДК 539.126.33  
ББК 22.382.912  
S11

**Sabirov B. M.**

S11 Muons and Nuclei, or the Adventures of the Muon in the Nucleus. —  
Dubna: JINR, 2024. — 36 p.

ISBN 978-5-9530-0615-6

The review describes the results of experiments based on quite different and independent approaches to solving the problem of interaction of muons with nuclei. Different paths of muon capture by nuclei and subsequent paths of secondary processes are considered: radiationless capture followed by nuclear fission, excitation of the nucleus with the escape of particles (neutrons and charged ones), and excitation of nuclear levels with the escape of gamma quanta. The experimental data require refinement, in particular with respect to the spectroscopy of fission fragments, the spectroscopy of secondary particles, and statistical accuracy. All of the experimental methods described rely on interpretation within theoretical models. Improvement in each of these parts will mutually stimulate refinements or new paths in subsequent research.

The article is addressed to young aspiring physicists interested in muon physics and looking for new phenomena of interactions of elementary particles with nuclei and atoms, and solutions to emerging problems using modern experimental methods.

**УДК 539.126.33**  
**ББК 22.382.912**

**ISBN 978-5-9530-0615-6**

© Joint Institute  
for Nuclear Research, 2024

*Dedicated to my wife Vera Pavlovna,  
a faithful friend and a reliable rear guard*

## **HISTORICAL BACKGROUND**

Of all the discovered elementary particles,  $\mu$  mesons from the very beginning were the most accessible for experimental study, since the bulk of cosmic radiation at sea level and even at mountain heights consists of strongly penetrating  $\mu$  mesons, which traverse significant layers of heavy matter, losing energy only for ionization. This particle was discovered in 1936 and was first called the mesotron by analogy with the positron discovered in 1933. The main properties of  $\mu$  mesons were studied even before the launch of large accelerators. After the discovery of the  $\pi$  meson and the phenomenon of  $\pi \rightarrow \mu$  decay, mesotrons were called  $\mu$  mesons. At the first stage of research, which began in 1936–1937, the phenomenon of  $\pi \rightarrow \mu \rightarrow e$  decay was discovered and the basic properties of  $\mu$  mesons were established. The second period in the experimental study of the properties of  $\mu$  mesons begins in 1948–1949 and is associated with the use of accelerators. Beams of  $\mu$  mesons created with accelerators allowed one to check, supplement and significantly improve the main results obtained earlier with cosmic radiation. New methods of research made it possible to obtain essentially new results. Thus, for example, during this period the spectroscopy of mesonic X-ray emission of  $\mu$ -meson atoms was developed, which gave impetus to extensive studies of mesoatomic and mesonuclear processes, and the interesting phenomenon of  $\mu$ -meson catalysis of the proton–deuteron fusion reaction was discovered. Since the end of 1956, a new period in the physics of  $\mu$  mesons has begun: new and completely unanticipated properties were discovered — the presence of  $\mu$ -meson longitudinal polarization, which made it possible to measure its magnetic moment, and then the property of depolarization of the muon spin allowed a huge series of studies of nuclear, atomic and even chemical properties of matter. The problem of depolarization is closely related to the discovery of a new hydrogen-like atom consisting of a  $\mu^+$  meson and an electron, called muonium. At the same time, it was confirmed with great accuracy that  $\mu$  mesons and electrons interact with the electromagnetic field equally [11] and thus the  $\mu$  meson began to be called “heavy electron”.

All the above-mentioned problems and properties of muons have been widely and comprehensively investigated at the Laboratory of Nuclear Problems using muon and pion beams of the Phasotron. Muon physics has its own peculiarity and advantage: during the research process the experimenter has the opportunity to work and communicate with an individual muon. The proposed review is devoted to one problem — the problem of muon capture by the nucleus. Experimental

work carried out at the Laboratory of Nuclear Problems and work that was carried out at the University of Bonn (Germany) with the participation of an LNP staff member are reviewed.

## INTRODUCTION

The study of interactions of mesons with complex nuclei yields important results relating to the properties of nuclei and the fundamental laws of strong, weak and electromagnetic interactions. The electromagnetic properties of the muon (charge, magnetic moment, etc.) are in complete agreement with the electromagnetic properties of the ordinary electron. With this identity, the mass of the muon is 200 times the mass of the electron. Therefore, in all electromagnetic processes, the muon behaves like a “heavy” electron.

The process of mesoatom formation can be divided into four conditionally independent stages. At the first one, the relativistic muons are slowed down by ionization to velocities comparable to those of electrons on the outer shell of the medium’s atoms. The deceleration time can be estimated using the well-known formula for ionization losses. For condensed media this estimate gives  $\tau_1 \approx \approx 10^{-9} - 10^{-10}$  s [1]. The second stage involves the final deceleration of muons to thermal velocities and adiabatic capture to higher-lying levels of the mesoatom, i.e., transition to a negative-energy state. Here the characteristic time  $\tau_2$  is  $10^{-13} - 10^{-14}$  s [2]. The third stage is the mesoatomic cascade, a process of muon transfer from high orbits to the ground state. The characteristic time of a mesoatomic cascade  $\tau_3$  in light nuclei does not exceed  $10^{-12} - 10^{-13}$  s, and in heavy nuclei it is even less [1]. The fourth stage is the stay of the muon in the  $K$  orbit of the mesoatom, culminating in its decay or nuclear capture. The muon lifetime in the  $K$  orbit  $\tau_4$  depends on the nuclear charge and varies from a free muon lifetime of  $2.2 \cdot 10^{-6}$  s in mesohydrogen to  $\sim 8 \cdot 10^{-8}$  s for the heaviest elements. This is due to the very strong dependence of the probability of  $\mu$  capture on the nuclear charge. Of the two competing processes, the decay is more likely in light nuclei, while at  $Z = 11$  (Na) their rates are comparable, and with increasing  $Z$  capture predominates [2, 3] (Fig. 1).

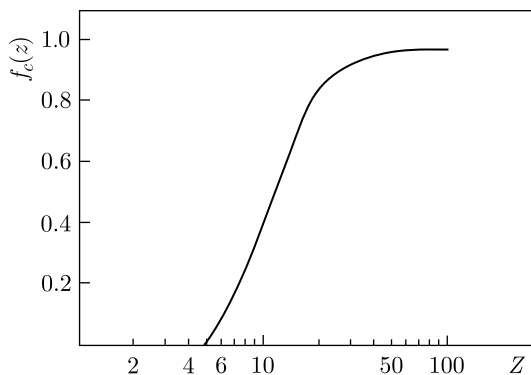


Fig. 1. Dependence of the relative muon capture rate on the nucleus charge  $Z$  [3]

The characteristic times  $\tau_1$ ,  $\tau_2$  and  $\tau_3$  of mesoatom formation are much shorter than the lifetime  $\tau_4$  of the muon in the  $K$  orbit. All events occurring at the first three stages can be considered prompt, while those at the fourth stage are delayed relative to the stopping of the muon in the target. It is known that muons trapped by the electric field of a nucleus, when moving to a lower energy level, emit quanta of energy, so-called muonic X rays, similar to the X rays emitted when an electron moves to a lower level in ordinary atoms, but much more energetic due to the muon's large mass.

## 1. RADIATIONLESS TRANSITIONS IN HEAVY MESOATOMS

As is well known, the capture of a  $\mu$  meson into the atomic orbit is a cascading process. The final stage of this process is the  $2p \rightarrow 1s$  transition in the  $\mu$  mesoatom. As a result of this transition, energy may be transferred to a gamma quantum, or (in heavy elements) a nucleus.

J.A. Wheeler [4] predicted two fission mechanisms of heavy nuclei by  $\mu^-$  mesons: "internal" fission, when the energy necessary for fission is released when the nucleus captures a muon from the lowest level of the mesoatom, and "external" fission, when the muon does not disappear, but the energy necessary for fission is released in a radiationless transition of the mesoatom to level  $1s$ .

The probability of non-radiative transfer of energy to the nucleus must be directly related to the photoelectric cross section on the nucleus. Since the lifetime of a  $\mu$  meson in the  $K$  orbit is much larger than that of a compound nucleus, the next stage of the process after the  $2p \rightarrow 1s$  transition is the decay of the excited nucleus. In particular, a fission process is possible if the transition energy is larger than the fission barrier. In the most favorable case, when the fission width is greater than all other nuclear widths, a catalytic nuclear fission process is possible. It should be noted that nuclear fission can occur not only as a result of non-radiative excitation of the nucleus, but also as a result of capture of a  $\mu$  meson from the  $K$  orbit of the nucleus — "internal" fission. These two fission mechanisms can be distinguished experimentally by the fact that in the first case fission is not accompanied by gamma quantum emission corresponding to the  $2p \rightarrow 1s$  transition. D.F. Zaretsky evaluated the effects associated with this process. As an example the nucleus  $^{238}\text{U}$  [5] was considered, because the greatest number of experimental data are available for it. Thus, the obtained estimate of the ratio of the probability of radiationless excitation  $W_b$  to the probability of emission of muonic X ray  $2p \rightarrow 1s$  radiation,  $W_\gamma$ , is

$$W_b/W_\gamma \approx 5-20.$$

So, the radiationless excitation process is more probable than radiation transition.

Several experimental works have been carried out to investigate the process of nuclear fission during muon capture using photoplates [6–8] and carried out using electronic methods of particle registration [16]. G.E. Belovitsky et al. (see Ref. [6]) concluded that stopping of  $\mu$  mesons in  $^{238}\text{U}$  led only to "internal" fission with a probability of 0.07; radiationless fission was not observed by the authors and has a probability less than 1%. In Ref. [8] M.G. Petrascu and

A. K. Mihul estimated the ratio of the probabilities of radiationless excitation ( $W_b$ ) and emission of  $\gamma$  quanta in  $2p \rightarrow 1s$  transition ( $W_\gamma$ ) for muon capture by a  $^{232}\text{Th}$  nucleus:

$$W_b/W_\gamma = 0.1 \pm 0.07.$$

It is suggested that in the case of thorium the excitation energy of the nucleus is transferred back to the meson, with the transition of the latter from the  $1s$  to the  $2p$  state being more probable than for uranium. J. A. Diaz et al. [9] also concluded that radiationless fission, if it occurs, should cause only a small fraction of the number of fission acts. D. F. Zaretsky [5] showed by his calculations that the probability of radiationless transitions in a uranium mesoatom, where the density of nuclear levels is high, must be significant. In the lead mesoatom with low density of nuclear levels (magic nucleus), this probability is practically equal to zero. Based on this work by Zaretsky, a group of physicists headed by B. Pontecorvo carried out an experiment to measure the yield difference of the corresponding radiative X-ray transitions in U and Pb [10]. Measurements were made using a muon beam of the JINR LNP synchrocyclotron, with a NaI(Tl) detector 30 mm in diameter and 35 mm high. Figure 2 shows photon spectra for mesouranium and mesolead in the energy range from 3 to 8 MeV.

The spectra are normalized to the same number of  $\mu$  mesons stopped in the target. The  $2p \rightarrow 1s$  transition energy in lead is  $E_\gamma = 6.02$  MeV, in uranium 200 keV less. Within the resolving power of the NaI(Tl) crystal, the peaks in the spectrum are quite close. The difference in photon intensities at energies  $\sim 6$  MeV in mesouranium and mesolead with identical geometry and

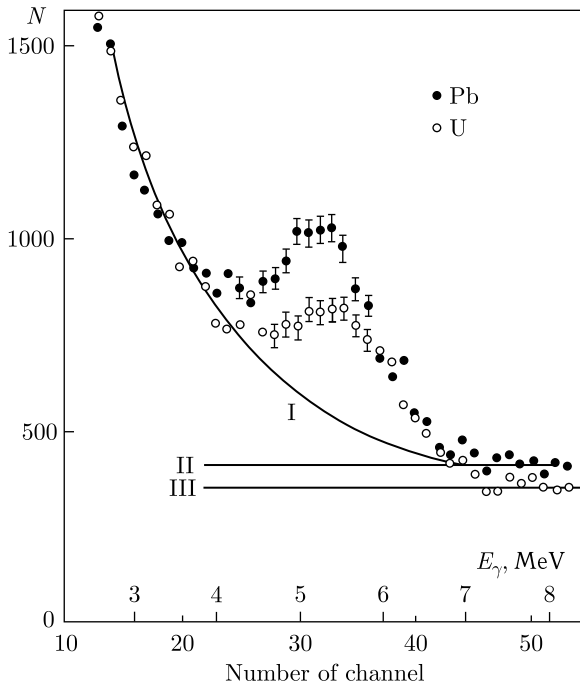


Fig. 2. Photon spectra from mesouranium and mesolead: I — interpolation of uranium and lead spectra; II — background level due to interpolation of uranium and lead spectra; III — rough background estimate obtained from the condition of equal widths of uranium and lead spectra

close emission energies indicates that the effect of radiationless transfer of  $\mu$  mesons to the  $1s$  mesouranium level is indeed observed here. Assuming that the radiationless transition probability in lead  $W_b$  is negligibly small compared with the probability  $W_\gamma$  of photon emission, the limits are obtained:

$$0.1 < (W_b/W_\gamma)U^{238} < 1.$$

Assuming that the widths of the uranium and lead peaks are the same, an estimate close to the lower limit of the inequality is obtained:

$$W_b/W_\gamma \sim 0.2.$$

The significance of the discovery consists primarily in the discovery of a new electromagnetic process in mesoatoms, in the possibility of studying the behavior of excited nuclei and the realization of nuclear reactions of a new type. The mechanism of nuclear reactions of this type was discussed in detail at the IV International Conference on High Energy Physics and Nucleus Structure, held in Dubna in 1971.

The discovery was included in the State Register of Discoveries of the USSR under the number 100 with the priority of June 17, 1959. The formula of the discovery states: "A previously unknown property of mesoatoms has been established, consisting in radiationless transfer of all the transition energy between mesoatom levels to the nucleus, when such an energy is close to the difference between the energies of nuclear levels".

Table 1. **Results of studies done in [47]**

Nucleus	$Y(2p \rightarrow 1s)$	Nucleus	$Y(2p \rightarrow 1s)$
	$Y(2p \rightarrow 1s)$		$Y(2p \rightarrow 1s)$
W	$1 \pm 0.08$	$^{235}\text{U}$	$0.71 + 0.05$
Pb	1	$^{238}\text{U}$	$0.77 + 0.04$
Th	$0.85 \pm 0.07$	$^{239}\text{Pu}$	$0.59 + 0.06$
Bi	$1 \pm 0.06$		

Further studies on radiationless transitions in heavy mesoatoms have been published in the literature [47] (see Table 1).

## 2. THE FATE OF THE MUON AFTER RADIATIONLESS NUCLEAR FISSION

Now it is interesting to trace the fate of the  $\mu$  meson after nucleus fission. There are two possibilities:

1) the  $\mu$  meson stays with the heavy fragment and perishes due to nuclear capture;

2) the  $\mu$  meson is also knocked off in the process of fission from the excited fragment.

One possible result of  $2p \rightarrow 1s$  (or  $3p \rightarrow 1s$ ) radiationless muon transition in a heavy mesoatom may be nuclear fission (so-called "prompt" fission [5]). This raises the question: what is the probability of detecting a muon in light or heavy fragments after fission? Several theoretical papers have estimated the probability

of detecting a muon in light and heavy fragments (10% and 90% obtained respectively by calculations in Ref. [11], and 50% and 50% in Ref. [12]). The results of Refs. [13, 14] qualitatively alter the original estimates of the probability of detecting a muon in light or heavy fragments. In muon problems, the finite size of the nucleus is of great importance. The use of the muon binding energy calculated in this work in the field of a finite-sized nucleus leads to a three- to fourfold increase in the muon transition probability to the nearest excited level of the fragment. The result of this work is that the average probability of detecting a muon in a light fragment (computed from the experimental distribution of fragments) is 1% and correspondingly 99% for a heavy fragment.

A meson ejection in the fission process is an unlikely event, because the flight of the fragments is slow compared to the muon velocity.

Another possible route for  $\mu$ -meson ejection is via the mechanism of internal conversion from an excited fragment. A theoretical evaluation of the internal conversion coefficient [11, 15] indicates that the electric dipole conversion coefficient for an average fragment excitation energy of  $\sim 10$  MeV is less than 1. This means that the  $\mu$ -meson ejection cannot compete with the emission of the first neutron from the fragment.

Recently, the probability of a muon sticking to light fragments has been measured at PSI. This experiment used a setup involving surface-barrier Si detectors to measure the kinetic energies of fragments, combined with the SINDRUM40 magnetic spectrometer consisting of five multiwire proportional chambers and a hodoscope. While Si detectors recorded fission fragments arising from radiationless transitions, SINDRUM40 detected electrons from muon  $\beta$  decay. This allows one to reconstruct the electron trajectories and hence to localize the region from which the electron from muon decay was emitted. As a result, one could determine whether the muon was attached to a light or to a heavy fragment. Thus, in addition to previously observed muon atoms of heavy fragments, muon atoms of light fragments decaying with lifetimes of  $(182 \pm 27)$  ns [39, 40] were also detected. From a preliminary analysis, the yield of muon atoms of light fragments was found to be  $0.057 \pm 0.007$ . Taking into account the probability of muon conversion to light fragments, the total yield of muon atoms of light fragments is found to be about 7%. At the same time, there are noticeable variations in the muon accession probability within the group of light fragments, ranging from  $0.015 \pm 0.015$  to  $0.090 \pm 0.027$  for mass windows of 77–87 and 107–117, respectively.

### **3. MUONIC X-RAY EMISSION FROM PROMPT FISSION FRAGMENTS**

After evaporation of the neutron, electromagnetic processes “come into play” and successfully compete with evaporation of the second neutron. In the presence of a bound muon, the following becomes possible: first, the conversion of  $\gamma$  rays on the muon [5, 11] and, second, the resonance process of radiationless enhancement of the muon energy up to an excited state with subsequent mesoatomic radiative transition [5, 15]. Theoretical predictions for the population

probability of the  $2p$  level of the muonic atom of a heavy fragment range from 1% to 10% per single fission event. These processes are quite possible because the experimental spectrum of  $\gamma$  rays of fission fragments extends up to 9 MeV [4], which significantly exceeds the muon binding energy of heavy (5.8 MeV) and light (3.3 MeV) fragments. D. F. Zaretsky and F. F. Karpeshin have considered resonance scattering of  $\gamma$  rays on a muon [11, 18].

To estimate the probability of muonic X-ray emission per one prompt fission (PF), the following circumstances are taken into account. Fission produces heavy fragments with atomic numbers in the interval  $Z = 51-57$  [17, 19] with a probability greater than 90%. For these elements, a change of  $Z$  by one, as the calculation shows, shifts the muonic X-ray line by 100 keV, so the total muonic X-ray spectrum of seven elements will occupy the interval of  $\approx 700$  keV.

In the spectrum of  $\gamma$  rays from PF fragments, there will be two lines corresponding to each isotope that are associated with resonant scattering of  $\gamma$  quanta on the muon and enhancement of its energy up to the intermediate states  $2p_{1/2}$  and  $2p_{3/2}$ , separated by  $\sim 60$  keV. The expected spectrum is shown in Fig. 3. The position of the lines is extremely sensitive to the charge distribution over the volume of the fragment: a change in  $r_0$  from 1.20 to 1.25 fm shifts the lines by 100 keV.

The observation of muonic X-ray radiation from a light fragment is hardly possible because of the low probability of muon capture by a light shard, which is about 1% [13]. As follows from experimental data [7], it is highly probable that the muon is propelled up to higher discrete states of the heavy fragment.

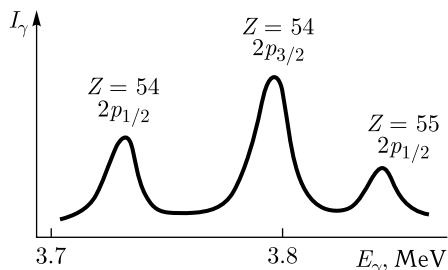


Fig. 3. Calculated shape of the hard part of the spectrum of  $\gamma$  radiation of prompt fission fragments

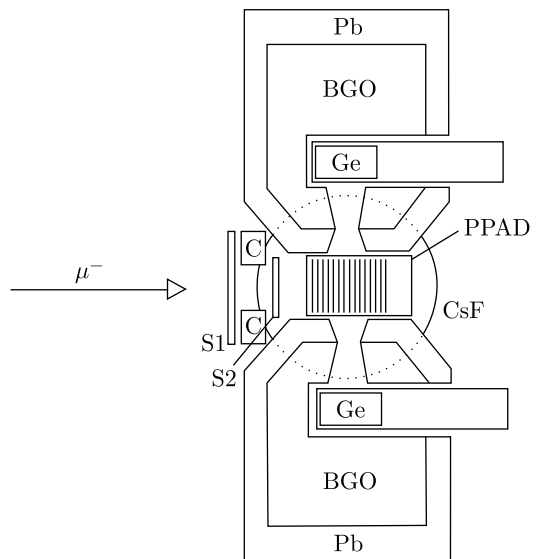


Fig. 4. Experimental setup: S1, S2 — scintillators; C — collimators; PPAD — fission detector; Ge — germanium detectors; CsF — CsF detector; BGO —  $\text{Bi}_4\text{Ge}_3\text{O}_{16}$  detectors; Pb — lead shield

Experimental study of muonic X-ray lines would give information on the multipolarity of hard  $\gamma$  transitions of nuclear fission fragments. Such an experiment was carried out at the University of Bonn by the group of Prof. P. David [20]. The experimental setup [23] consisted of two germanium detectors to detect X rays and an avalanche counter with several parallel plates filled with  $^{238}\text{U}$  metal foil, which served as the active target (Fig. 4).

Muonic X rays from a  $^{238}\text{U}$  target were recorded in coincidence with both prompt and delayed fission fragments. The muonic X-ray spectrum coinciding with prompt fission also had to contain muonic X-ray emission from fission fragments. The energies of both lines of the  $2p \rightarrow 1s$  transition complex of the most likely isotope  $^{140}\text{Xe}_{54}$  are 3.7 and 3.8 MeV, respectively. Because of the charge distribution, the  $2p \rightarrow 1s$  transitions of muon heavy fragments should be within the energy range of about 700 keV [18]. Additional complexity arises from the mass distribution. Furthermore, Doppler broadening smears out the separate lines [21]. Figure 5 shows the spectrum recorded in coincidence with the PF of one of the high-purity Ge diodes.

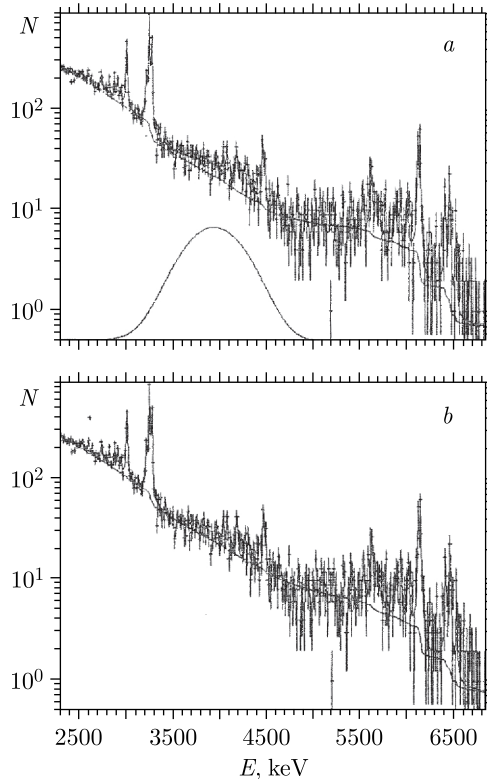


Fig. 5. The muonic X-ray spectrum recorded by a single Ge detector in coincidence with the PF in the  $^{238}\text{U}(\mu^-, \gamma f)$  experiment [23]. The full lines show the fit to this spectrum, the background and the Gaussian curve. The upper spectrum (a) contains the fit with a broad Gaussian structure at 3910 keV, the lower spectrum (b) is without such a structure

A broad structure can be visualized in the energy region between the  $3d \rightarrow 2p$  and  $2p \rightarrow 1s$  muon transitions of  $^{238}\text{U}$ , and it appears to be a suitable candidate for muon  $2p \rightarrow 1s$  transitions of muons trapped by heavy fragments and made to occupy discrete states. Thus, an attempt has been made to fit this spectrum using the FIT program [22] over a wide energy range, taking into account all muonic X-ray lines and the background as described in [23]. A Gaussian function was used to describe the observed total structure. The fitting for the spectrum of one detector is shown in Fig. 5. The final results were obtained from the data measured by both Ge detectors. The position of the conglomerate was determined to be  $(3910 \pm 40)$  keV with a width of  $(640 \pm 110)$  keV (FWHM). The intensity  $I_s$  of this conglomerate with respect to the intensity  $I_{\text{pf}}$  observed during the prompt fission was determined to be  $I_s/I_{\text{pf}} = (6.0 \pm 2.1)\%$ . Although the experimental value for the occurrence of this phenomenon is weak, it is still the first experimental indication of its existence.

#### 4. SYSTEMATICS OF THE ABSOLUTE YIELDS FOR HEAVY NUCLEI AFTER FISSION IN THE CASE OF $\mu^-$ CAPTURE

To systematize the yields of the various reactions such as fission or neutron emission after the excitation process, the fraction of radiationless muon transitions that directly excite the nucleus must be known. This fraction for  $2p \rightarrow 1s$  transitions can be defined as the difference between the occupancy of the  $2p$  level and the intensity of  $2p \rightarrow 1s$  radiation transitions. In the works by B. Pontecorvo [10] and J. A. Diaz [30], only a qualitative estimation of the fraction of radiationless transitions in actinide nuclei is given by the decrease in the intensity of  $2p \rightarrow 1s$  transitions in thorium, uranium and plutonium as compared to the intensity of this transition in the magic lead nucleus. It was assumed that the intensity of higher radiation transitions in these nuclei must be equal. Otherwise the missing part of the intensity of  $\gamma$  rays cannot be simply related to radiationless transitions. To verify these assumptions, a group led by S. M. Polikanov has systematically investigated the fission of heavy nuclei in the case of  $\mu$ -meson capture:  $^{232}\text{Th}$ ,  $^{238}\text{U}$ ,  $^{235}\text{U}$ ,  $^{237}\text{Np}$ ,  $^{242}\text{Pu}$  and  $^{239}\text{Pu}$  [24–27]. Nuclear fission due to  $\mu$ -meson capture differs from other types of fission [37, 38], because it proceeds with a characteristic average lifetime of about 80 ns and the average excitation energy of the nucleus is estimated to be 15–20 MeV [28]. This is sufficient to open the fission channel in the de-excitation modes of the nucleus. The excitation of a nucleus in the radiationless transition of a muon to the  $K$  orbit occurs within a time interval characteristic of muon cascading, such as  $10^{-14}$ – $10^{-15}$  s from the moment of  $\mu$ -atomic capture [4]. It is therefore called the prompt fission process. There are some features that are of great interest in terms of fission barrier research. Figure 6 shows the experimental setup together with a block diagram of the recording electronics [36].

A fast multi-plate ionization chamber filled with methane was used in the experiment. The control measurement of the fast coincidences  $f$ – $\gamma$  had a resolution time of 2.5 ns. The fission fragments were recorded with an efficiency

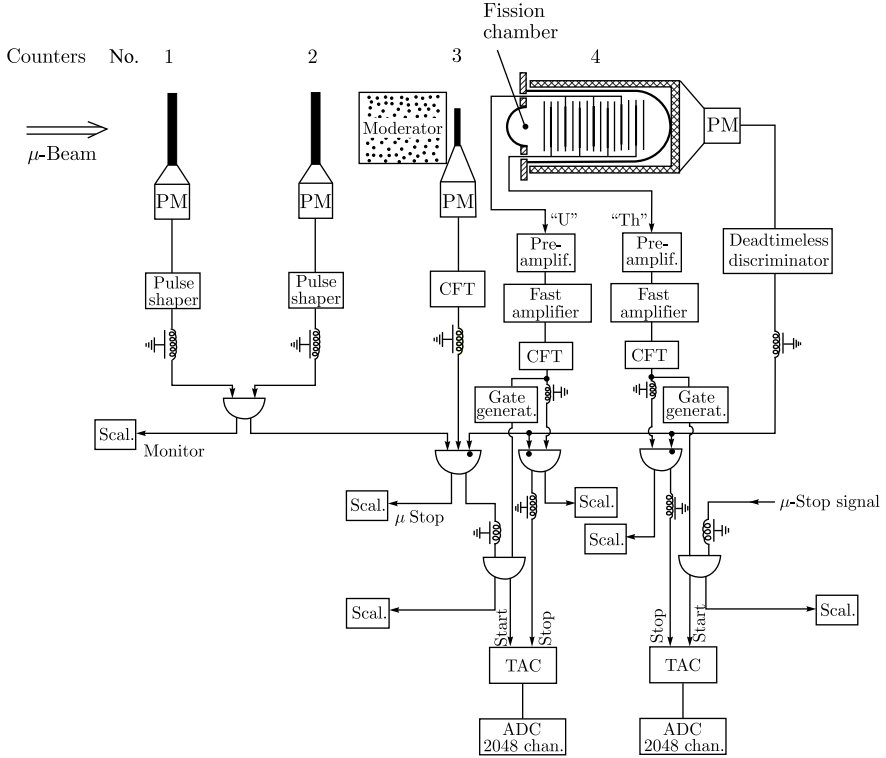


Fig. 6. Block diagram of the electronics used in conjunction with the fission chamber and telescope counters

of at least 90%. All measurements were carried out simultaneously for two isotopes: the test and  $^{238}\text{U}$  as a reference. The targets were deposited by sedimentation on aluminium foils about  $13 \text{ mg/cm}^2$  thick. Natural uranium  $^{238}\text{U}$  and  $^{235}\text{U}$  (95% isotopic purity) were deposited as  $\text{U}_3\text{O}_8$  oxides. The thorium target (monoisotope  $^{232}\text{Th}$ ) was fabricated as  $\text{ThO}_2$  oxide. The targets were prepared as discs 47 mm in diameter and 2.6, 0.7 and  $3.1 \text{ mg/cm}^2$  thick for  $^{238}\text{U}$ ,  $^{235}\text{U}$  and  $^{232}\text{Th}$ , respectively. When measured, the chamber contained 857 mg  $^{238}\text{U}$ , 237 mg  $^{235}\text{U}$ , and 1020 mg  $^{232}\text{Th}$ .

The measurements were carried out with  $\mu^-$ - and  $\pi^-$ -separated beams of the JINR LNP synchrocyclotron at  $E_p = 680 \text{ MeV}$ . The  $\mu^-$  beam of 98% purity with an average energy of 85 MeV and dispersion  $\Delta E = 9 \text{ MeV}$  was slowed down in a moderator of  $30 \text{ g/cm}^2$  equivalent thickness. By measuring the time distribution of the induced fission, the ratios of prompt and delayed fission and the induced fission yields of  $^{232}\text{Th}$  and  $^{235}\text{U}$  in relation to the fission yield of  $^{238}\text{U}$  were obtained. To control the stability of the timing system and to analyze the response curves of the fast coincidences, measurements with  $\pi^-$  mesons were made periodically for each measurement cycle (Fig. 7).

The relative fission probabilities of fission induced by  $\pi^-$  mesons of  $^{232}\text{Th}$ ,  $^{235}\text{U}$  and  $^{238}\text{U}$  were obtained:  $(43 \pm 3)\%$ ,  $(120 \pm 5)\%$  and 100%, respectively. Using literature data on the measurement of the fission probability of  $^{238}\text{U}$

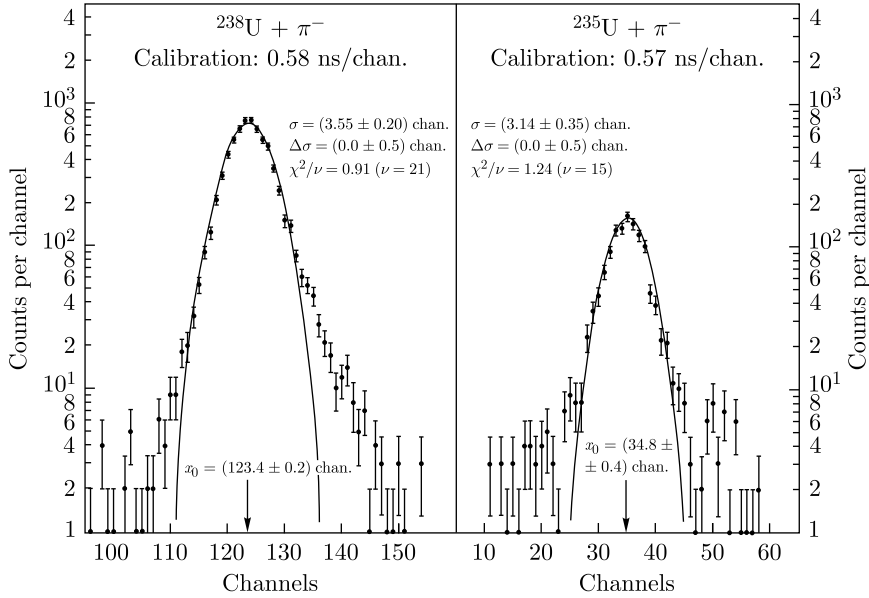


Fig. 7. Two examples of the time distribution of fission induced by  $\pi^-$  mesons

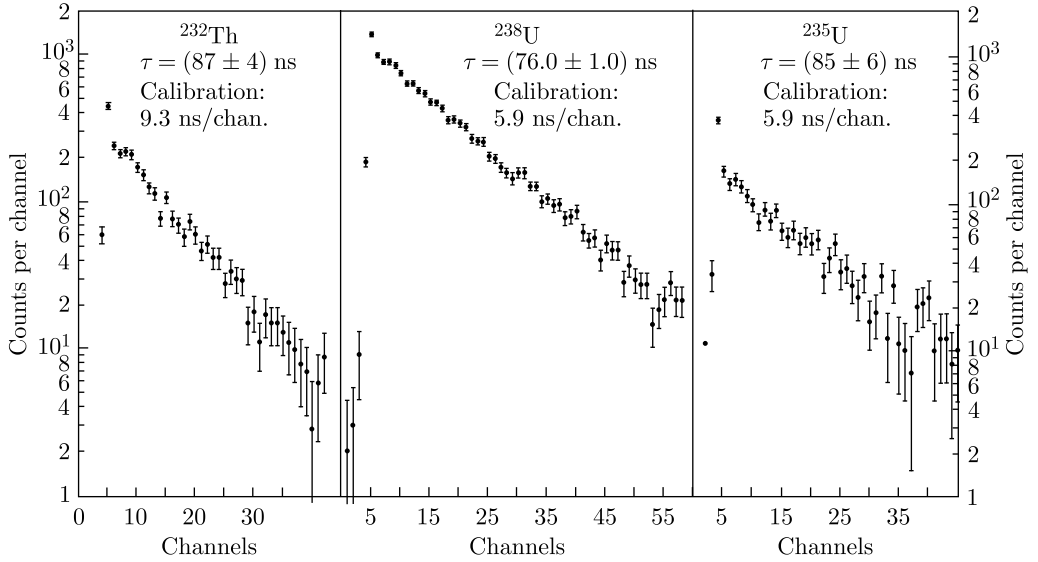


Fig. 8. Time distribution of fission events in  $^{232}\text{Th}$ ,  $^{238}\text{U}$  and  $^{235}\text{U}$  induced by  $\mu^-$  mesons (background has been subtracted)

induced by  $\pi^-$  mesons [28] and adopting the mean value  $0.45 \pm 0.10$  as a basis, the values  $0.22 \pm 0.05$  for  $^{232}\text{Th}$  and  $0.54 \pm 0.12$  for  $^{235}\text{U}$  were obtained. The time distributions of fission events induced by  $\mu^-$  in the three isotopes studied are shown in Fig. 8.

The weighted prompt versus delayed fission yield ratios for the three measured isotopes are compared with the results from [29–31]. There is a

Table 2. **The prompt and delayed fission yields per  $\mu^-$  capture [24]**

Type of fission	Fission yield per $\mu^-$ capture		
	$^{232}\text{Th}$	$^{238}\text{U}$	$^{235}\text{U}$
Prompt	$(5.0 \pm 1.2) \cdot 10^{-4}$	$(2.03 \pm 0.45) \cdot 10^{-3}$	$(5.1 \pm 1.2) \cdot 10^{-3}$
Delayed	$(3.8 \pm 0.9) \cdot 10^{-3}$	$(2.90 \pm 0.65) \cdot 10^{-2}$	$(3.2 \pm 0.8) \cdot 10^{-2}$

discrepancy for  $^{232}\text{Th}$  and  $^{235}\text{U}$ . From a compilation of all available fission yield data on  $\mu^-$  capture [6, 8, 29–31], the final experimental results for the absolute probabilities of prompt and delayed fission yields are obtained. These are shown in Table 2.

Omitting all theoretical speculations, the main conclusions from the measurement results can be given:

1) in  $^{238}\text{U}$  and  $^{235}\text{U}$  the prompt fission is induced mainly by  $K_\alpha$  radiationless transitions; in  $^{232}\text{Th}$  other higher radiationless transitions may contribute significantly;

2) there is a strong lessening of the photofission probability of nuclei with a muon in the  $1s$  orbit; i.e., the probability of photofission of the nuclei examined with a muon in the  $1s$  orbit  $P_{f\mu}$  is much lower than that of  $P_{f0}$  (without a muon in the  $1s$  orbit);

3) there is a fairly sharp change in the  $P_\mu/P_0$  ratio from one nucleus to the other, while for  $P_0$  alone there is little change.

It seemed interesting to extend the systematics to include such nuclei as  $^{239}\text{Pu}$ ,  $^{242}\text{Pu}$  and  $^{237}\text{Np}$ . And so the following study was devoted to investigating the absolute yields for these three additional isotopes, two of which,  $^{237}\text{Np}$  and  $^{242}\text{Pu}$ , had not been studied [25]. The experimental setup, measurement procedure and analysis were identical to those given above. The measurements were carried out using  $\mu^-$  and  $\pi^-$  separated synchrocyclotron beams at the JINR Laboratory of Nuclear Problems at 680 MeV. Fission events were recorded in a fast multi-plate ionization chamber filled with methane. The  $\mu^-$ -stop events were recorded by a telescope counter consisting of four plastic scintillators operating in the ordinary coincidence mode of  $123\bar{4}$ . The chamber contained  $(111 \pm 6)$  mg  $^{237}\text{Np}$ ,  $(7.70 \pm 0.85)$  mg  $^{242}\text{Pu}$  and 125 mg  $^{239}\text{Pu}$ . The detection efficiency was (95–100)% in measurements with  $^{237}\text{Np}$  and  $^{242}\text{Pu}$ , and  $(52 \pm 5)\%$  in the case of  $^{239}\text{Pu}$ . The time distributions of fission events with respect to the stopping point were measured simultaneously for the following isotope pairs:  $^{237}\text{Np}$  and  $^{238}\text{U}$ ,  $^{239}\text{Pu}$  and  $^{235}\text{U}$ ,  $^{242}\text{Pu}$  and  $^{239}\text{Pu}$ . From the relative fission yields, absolute yields can be obtained using the values for  $^{238}\text{U}$  and  $^{235}\text{U}$  given in Ref. [24].

The measured spectra summed over all 16 channels are shown in Fig. 9. The mean decay time was found by the least square method with a confidence level of 0.05.

The primary spectra were fitted using the prompt coincidence response curve determined in  $\pi^-$  measurements and its convolution with an exponential decay curve and a constant background. This procedure resulted in relative yields for the two types of fission and fission probability ratios for the studied nuclei. The absolute yields for  $\pi^-$  capture were found using the values for  $^{238}\text{U}$  and  $^{235}\text{U}$

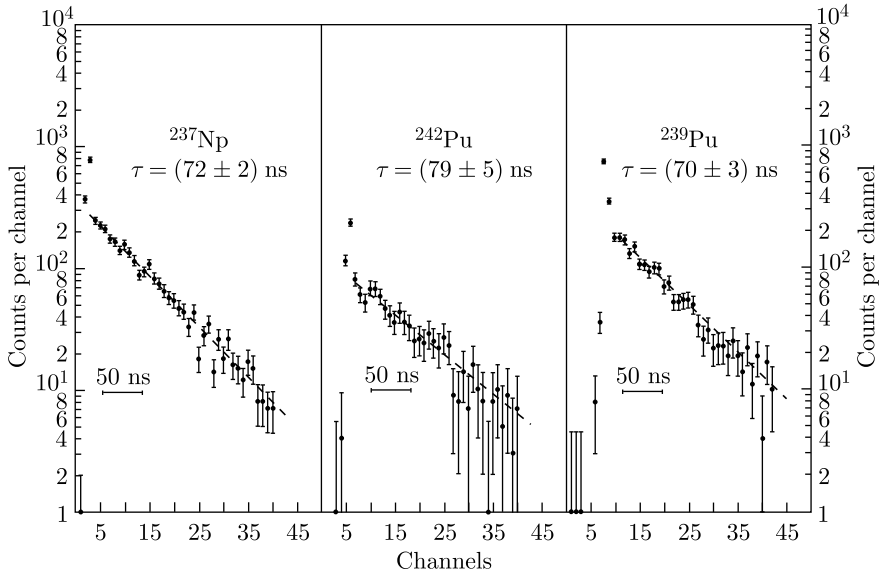


Fig. 9. Time distribution of fission events in  $^{237}\text{Np}$ ,  $^{242}\text{Pu}$ , and  $^{239}\text{Pu}$  induced by  $\mu^-$  (background subtracted). The drawn lines indicate the fit of the exponential decay curve to the data points. Calibration: 6.84, 5.8, and 6.14 ns/channel for  $^{237}\text{Np}$ ,  $^{242}\text{Pu}$ , and  $^{239}\text{Pu}$ , respectively

given in [24]. The results are shown in Fig. 10 together with the photofission probability for the photon energy corresponding to the energy of the  $2p \rightarrow 1s$  muon transition in these nuclei.

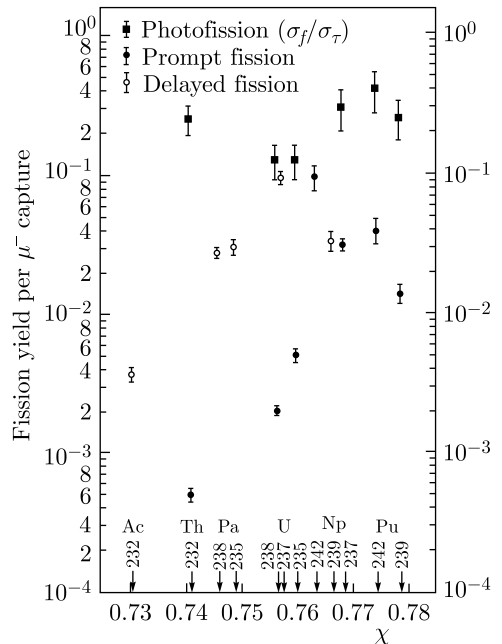


Fig. 10. Absolute yield for prompt and delayed fission caused by  $\mu^-$  capture as a function of the separability parameter  $\chi$  [32]

Conclusions as the follows:

- a) the prompt fission yield is much smaller than the photodetachment probability and shows a pronounced change with the fission parameter  $\chi$ ;
- b) the probabilities of fission induced by trapped muons (delayed fission) are several times lower than predicted from the systematic  $\Gamma_p/\Gamma_f$  ratio, as far as is currently known for the 15–20 MeV nuclear excitation characteristic of  $\mu^-$  trapping.

Thus, by measuring the relative yields of fission events, absolute yields could be obtained using the corresponding values for  $^{238}\text{U}$  and  $^{235}\text{U}$  published in [24]. Fission induced by  $\pi^-$  reproduces only prompt events, and measurements with a  $\pi^-$  beam allow the characteristics of the timing system to be controlled and the response curve of the prompt coincidence to be analyzed for each measurement independently together with the photon separation probability for the photon energy corresponding to the  $2p \rightarrow 1s$  muon transition energy in these nuclei (see Fig. 10). The yields for the prompt fission, normalized to the emissionless transition probabilities, were taken from [24].

In this analysis, it has been assumed that the energy spectra of the fragments are the same for prompt and delayed fission. The prompt fission yield is much lower than the photofission probability and shows a pronounced change with the fissibility parameter  $\chi$  [41–43].

Knowing the intensity of muonic X-ray transitions is important for studying the properties of muon atoms. The fraction of radiationless muon transitions directly exciting the nucleus for  $2p \rightarrow 1s$  transitions can be defined as the difference between the  $2p$  level occupancy and the intensity of radiation transitions  $2p \rightarrow 1s$ . In order to check these assumptions, an experiment for measurement of the intensities of the main muonic X-ray lines in lead, thorium and uranium was carried out [27]. The experiment was carried out with the separated beam of negative muons of JINR LNP synchrocyclotron ( $E_p = 670$  MeV). The muonic X-ray radiation was recorded using a coaxial Ge(Li) detector with a  $45 \text{ cm}^3$  sensitive volume, in coincidence with the stopping signal in the target. The time resolution of  $2\tau$  was 10 ns, while the energy resolution of the Ge(Li) detector was 3 and 8 keV for gammas with energies of 1 and 8 MeV, respectively. All targets had the same dimensions of  $60 \times 77$  mm, their weight was approximately 50 g, and their effective thickness was  $\approx 2 \text{ g/cm}^2$ . Of great importance for the present experiment was the reliable determination of the  $\gamma$ -ray registration efficiency and of the number of  $\mu^-$  stops in the target. In order to reduce errors associated with the possible beam instability, ten measurement cycles were carried out. In each cycle, six measurements were carried out with four targets in the following order: Al, Pb, Al, Th, Al, U. In this way, an effective averaging of the beam fluctuations was achieved. The efficiency curve of the Ge(Li) detector was normalized to absolute units by the known  $K_\alpha$  muonic X-ray line intensity in Al [33].

The measurements were carried out in two stages. First, the intensities of  $6h \rightarrow 5g$  and  $5g \rightarrow 4f$  transitions in Pb, Th, U were determined; then muonic X-ray spectra of all targets in the range from 150 keV to 7 MeV were measured

Table 3. Intensity of radiative muonic transitions

Transition	Pb(nat)			$^{232}\text{Th}$			$^{238}\text{U}$		
	$E$ , keV	$I_{\text{exp}}$	$I_{\text{calc}} (\alpha = -0.14)$	$E$ , keV	$I_{\text{calc}}$	$E$ , keV	$I_{\text{exp}}$		
$\Sigma 7i \rightarrow 6h$						166–182	$0.367 \pm 0.025$		
$9j \rightarrow 7i$									
$9i \rightarrow 7h$				181–191	$0.034 \pm 0.004$	190–200	$0.040 \pm 0.004$		
$8i \rightarrow 6h$						285–295	$0.043 \pm 0.007$		
$\Sigma 6h \rightarrow 5g$	230–237	$0.436 \pm 0.0355$	0.405	274–291	$0.315 \pm 0.022$	285–304	$0.391 \pm 0.027$		
$7h \rightarrow 5g$	370–375	$0.060 \pm 0.005$	0.075	443–456	$0.035 \pm 0.0033$	464–477	$0.050 \pm 0.006$		
$5g_{9/2} \rightarrow 4f_{7/2}$	429–432	$0.265 \pm 0.016$	0.239		$0.176 \pm 0.014$		$0.228 \pm 0.016$		
$5g_{7/2} \rightarrow 4f_{5/2}$	437–441	$0.192 \pm 0.013$	0.211		$0.139 \pm 0.009$		$0.173 \pm 0.010$		
$\Sigma 5g \rightarrow 4f$	429–441	$0.457 \pm 0.032$	0.450	514–535	$0.315 \pm 0.022$	537–560	$0.401 \pm 0.026$		
$6g \rightarrow 4f$	662–673	$0.055 \pm 0.005$	0.080	794–816	$0.033 \pm 0.004$	831–854	$0.048 \pm 0.005$		
$4f_{5/2} \rightarrow 3d_{5/2}$	929	$0.024 \pm 0.003$	0.916						
$4f_{7/2} \rightarrow 3d_{5/2}$	938	$0.298 \pm 0.021$	0.320	1115–1151	$0.205 \pm 0.015$	1170–1210	$0.260 \pm 0.020$		
$4f_{5/2} \rightarrow 3d_{3/2}$	995–972	$0.224 \pm 0.016$	0.284	1174–1193	$0.135 \pm 0.010$	1230–1260	$0.180 \pm 0.012$		
$\Sigma 4f \rightarrow 3d$		$0.546 \pm 0.040$	0.570		$0.340 \pm 0.025$		$0.440 \pm 0.032$		
$3d_{5/2} \rightarrow 2p_{3/2}$	2501	$0.298 \pm 0.022$	0.435	2730–2740 2792–2825	$0.074 \pm 0.012$	2810–2850 2860–3035	$0.142 \pm 0.020$		
$3d_{3/2} \rightarrow 2p_{1/2}$	2642	$0.176 \pm 0.014$	0.245	3088–3157	$0.159 \pm 0.013$	3215–3242	$0.185 \pm 0.020$		
$\Sigma 3d \rightarrow 2p$		$0.474 \pm 0.0383$	0.680		$0.233 \pm 0.025$		$0.327 \pm 0.040$		
$2p_{1/2} \rightarrow 1s_{1/2}$	5781	$0.259 \pm 0.026$	0.295	6000–6120	$0.230 \pm 0.024$	6050–6200	$0.312 \pm 0.030$		
$2p_{3/2} \rightarrow 1s_{1/2}$	5967	$0.336 \pm 0.029$	0.585	6280–6470	$0.230 \pm 0.024$	6380–6580	$0.237 \pm 0.024$		
$\Sigma 2p \rightarrow 1s$		$0.595 \pm 0.060$	0.880		$0.460 \pm 0.048$		$0.550 \pm 0.055$		

for a long time and the relative intensities of transitions were determined. The final results of these measurements are shown in Table 3. The photopeak relative detection efficiency curve has been determined using known calibration sources and the  $^{35}\text{Cl}(n, \gamma)$  reaction. For functional representation of this curve by means of the polynomial of the fourth degree in twice logarithmic coordinates ( $\log \varepsilon\gamma, \log E\gamma$ ), the error corridor with a relative width of 0.5% was calculated. The gamma-ray spectra were processed using the SAMPO software [34]. Then, in Fig.11 the experimental results were compared with the predictions of cascade calculations according to the Hufner program [35]. The calculations took into account radiative  $E1$  transitions and Auger transitions, and, also, electron conversion on  $K, L, M$  shells, and the initial occupancy for  $n = 20$  was assumed to have the form  $\rho \sim (2l + 1) \exp(\alpha l)$ .

The experimental and theoretical values of intensity of transitions  $6 \rightarrow 5$ ,  $5 \rightarrow 4$  and  $4 \rightarrow 3$  in lead coincide at  $\alpha = 0.14$ . But for such a value of  $\alpha$ , the calculated intensities of transitions  $3 \rightarrow 2$  and  $2 \rightarrow 1$  are much larger than the experimental values. Moreover, for uranium and thorium the agreement between the calculated and experimental values cannot be achieved at any value of  $\alpha$ . From these measurements we can conclude that the intensities of the corresponding transitions for lead and actinides are markedly different.

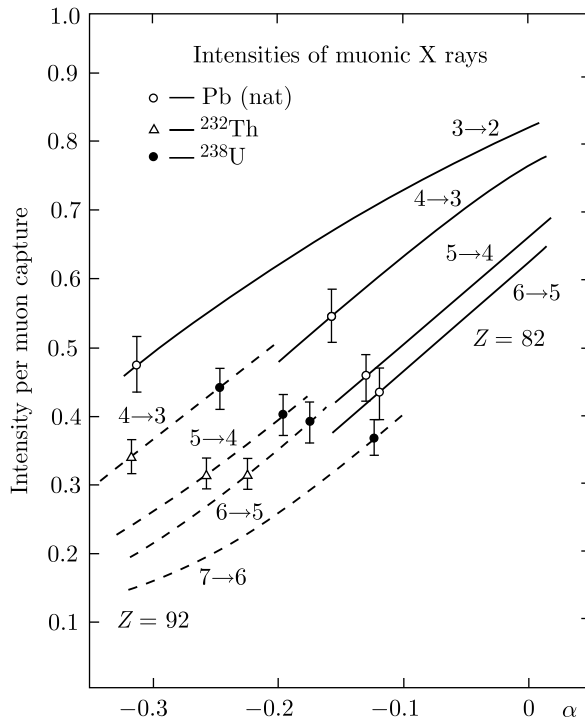
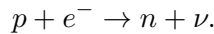


Fig. 11. Results of cascade calculation of intensity of muon transitions per act of  $\mu^-$  capture for  $Z = 82$  and  $92$ . The dependence of the transition intensity on the parameter  $\alpha$  of the initial distribution is presented:  $\rho \sim (2l + 1) \exp(\alpha l)$ . Dashed lines show the measurement results

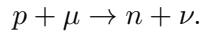
Consequently, the decrease in muonic X-ray intensity cannot be attributed solely to the fraction of radiationless transitions. Apparently, this indicates that the mentioned assumptions of cascade calculations concerning the initial population in muon atoms are incorrect. In addition, it is possible that these calculations do not reproduce the observed intensity because they do not take into account the coupling between nuclear and atomic motions. For a reliable determination of the fraction of radiationless transitions, it is necessary, first, to improve the theoretical methodology for calculating the process of muon cascading and, second, to measure more carefully the difference between the probabilities of occupying muon states and of their radiation decay, which requires a significant increase in the sensitivity of the measurement.

## 5. NEUTRON EMISSION IN THE CASE OF NUCLEAR $\mu^-$ CAPTURE

B. Pontecorvo [44] (1950) assumed that the interaction of a  $\mu^-$  meson with a nucleus may be described by analogy with  $K$  capture in nuclear  $\beta$  decay. The capture by the nucleus of an orbital electron is described by the reaction

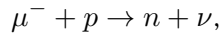


Similarly, a  $\mu$  meson in the  $K$  shell of a mesoatom can be captured by a nuclear proton. As in the above reaction, the proton will turn into a neutron and a neutrino will be emitted:



For the first time (1962), the  $\mu^-$ -meson capture reaction was observed directly in a liquid hydrogen bubble chamber in a well-purified beam of  $\mu^-$  mesons at the Chicago accelerator (99% of  $\mu^-$  mesons, the  $\pi^-$ -meson contamination was about 0.5%). The neutrons produced in this reaction should have energies close to  $\approx 5.2$  MeV [45, 46]. The data obtained by measuring the spectrum of neutrons arising from stopping  $\mu^-$  mesons in the chamber are shown in Fig. 12 (the background measurements are subtracted from these data).

Thus, the results of the experimental study of the interaction of  $\mu^-$  mesons with the simplest nuclei have been summarized, and the first theoretical justification of the mechanism of nuclear  $\mu$  capture has been given. From the data considered, it followed that the interaction of a  $\mu^-$  meson with nuclear matter can be explained by the reaction



in which the proton that absorbed the  $\mu^-$  meson transforms into a neutron, and nearly all the energy released in this process, close to the  $\mu^-$ -meson rest energy, is carried away by neutrinos.

If a  $\mu^-$  meson is captured by a proton at rest, the energy of the neutron is close to 5.2 MeV. Due to the nucleon motion in the nucleus, the neutron energy turns out to be noticeably higher and can reach several tens of megaelectronvolts. A fast neutron either leaves the nucleus or knocks a particle out of the nucleus in actual interaction, or it transfers its energy to intranuclear nucleons, "heating up" the nucleus. The secondary particles produced in the nuclear capture reaction

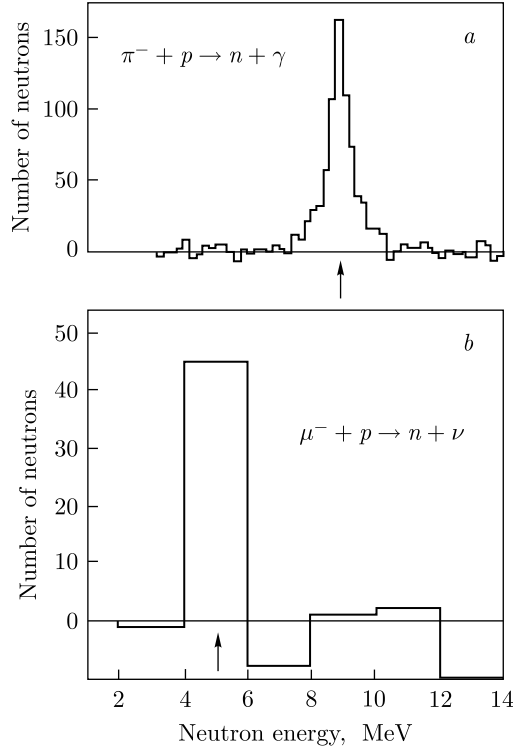
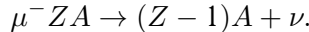


Fig. 12. Neutron energy spectrum from the reaction  $\pi^- + p \rightarrow n + \gamma$  (performed for calibration) (a) and from the reaction  $\mu^- + p \rightarrow n + \nu$  (Hildebrand experiment [45]) (b)

of the muon are the neutrino and neutron. The absorption of a  $\mu^-$  meson by a proton reduces the charge of the nucleus by one:



In the first experiments, neutron counters used to register neutrons were in the form of proportional counters filled with  $\text{BF}_3$ , enriched  $^{10}\text{B}$  trifluoride boron. For greater efficiency, in other works a liquid scintillator with cadmium introduced into it was used. The ultimate goal of the measurements was to record the multiplicity of emitted neutrons  $\bar{n}$  (see Table 4).

For a long time it was believed that absorption of the muon by a nucleus was due to its interaction with one of the protons of the nucleus, while all the other nucleons — protons and neutrons — acted only as an external medium, in which the elementary act of converting the proton–muon pair into a neutron–neutrino pair occurred [49, 50]. In 1963, a group of theorists from the Institute of Nuclear Physics of Moscow State University and the Laboratory of Theoretical Physics of the Joint Institute for Nuclear Research, headed by Professor V. V. Balashov, put forward a fundamentally different model of the process, which was based on the idea that absorption by the nucleus is of a multi-particle collective nature. A mathematical theory of the phenomenon was developed, and directions for its experimental study were indicated [47].

Table 4. **Average number of neutrons  $\bar{n}$  (multiplicity) per capture of  $\mu^-$  meson by a nucleus [46]**

Nucleus	$Z$	$\bar{n}$	Method
Na	11	$1.0 \pm 0.4$	Boron counters for slow neutrons, magnetic analysis of $\mu^-$ -meson sign
Mg	12	$0.6 \pm 0.2$	Boron counters for slow neutrons
Al	13	$0.95 \pm 0.17$	Boron counters for slow neutrons
Ca	20	$0.40 \pm 0.4$	Same
Ag	47	$1.55 \pm 0.06$	Liquid scintillator with Cd for neutron counting
Sn	50	$1.54 \pm 0.12$	Boron counters for slow neutrons
I	57	$1.7 \pm 0.4$	Radiochemical method: search for tellurium isotopes
		$1.49 \pm 0.06$	
Pb	82	$2.14 + 0.13$	Boron counters for slow neutrons
		$1.64 \pm 0.07$	
		$1.70 \pm 0.30$	
		$1.50 \pm 0.40$	Same
		$1.96 \pm 0.72$	Boron counters for slow neutrons
		$2.32 \pm 0.17$	
Au	79	$1.63 \pm 0.06$	

In the problem of  $\mu^-$  capture, two problems are closely intertwined: the first, related to the physics of elementary particles, is the understanding of the nature of the fundamental interaction on the basis of the proposed theory of the Universal Fermi Interaction (UFI), and the second is the study of the structure of the nucleus by means of  $\mu^-$  mesons. In analyzing experimental data, the nucleus was considered to make negligible changes in characteristics of the elementary act of capture, and these changes were considered to be accounted for applying the simplest models of nuclei. The abundance of different experimental data led to formulation of the idea of giant resonance excitation in the nuclei during the capture of  $\mu^-$  mesons. The main channel in the capture of  $\mu$  mesons by nuclei is the neutron escape channel. The decisive role in determining the interaction of the escaping neutron with the residual nucleus at energies of the order of several megaelectronvolts is played by a proton hole that appears in one of the nuclear shells as a result of the absorption of the  $\mu^-$  meson. The particle-hole interaction leads to changes in the state of the residual nucleus and, eventually, to coherent excitation of various degrees of freedom of the nucleus corresponding to individual partial-hole configurations; a collective excited state of the nucleus, the giant resonance, appears [51]. Excitation of the giant resonance is not specific to the process of  $\mu$ -meson capture, but is a universal property of the nucleus. Collective states, excited in this process, decay into different levels of the oscillating nucleus and form the neutron spectrum. Thus, the basis of modern ideas on the general properties of nuclear transitions into a continuous spectrum during  $\mu$  capture is the idea of a resonant, collective mechanism of muon absorption by the nucleus. In [47] a hypothesis was put forward concerning the modes of decay of quasi-bound states of the intermediate nucleus. According to this hypothesis, the energy of such states may (at least in the case of light

nuclei) be concentrated on a single nucleon, most commonly a neutron. Neutron energy spectra calculated using this approach have a characteristic line form where each line corresponds to a transition between one of the quasi-bound states of the intermediate nucleus and one of the states of the final nucleus produced by the neutron escape.

To check the theoretical predictions, at the Laboratory of Nuclear Problems, a series of experiments was performed under the guidance of V.S. Evseev for the measurement of neutron yields from various nuclei during  $\mu$  capture, to measure their energy spectra and to search for the line structure of neutron spectra [52–54].

The work was carried out with a pure muon beam with a momentum of 158 MeV/c, obtained using the meson channel of the synchrocyclotron of the JINR Laboratory of Nuclear Problems. The arrangement of the apparatus is shown in Fig. 13. The muon stops are isolated according to the standard 1234 scheme (scintillator counters 1–4 in Fig. 13). Distilled water targets M in a thin container of polystyrene foam, molten sulfur, calcium metal and lead metal had an area of  $100 \times 100$  mm and a thickness (towards the neutron spectrometer 5) of 2, 4, 4 and 6 g/cm<sup>2</sup>, respectively.

A stilbene crystal 30 mm in diameter and 20 mm thick with a photomultiplier tube 56 AVP [55] was used as the neutron detector 5. The pulse shape discrimination method was used to separate neutrons and gammas [55, 56]. The coincidences in time between the pulses of the neutron detector and the pulses of  $\mu^-$  stops triggered a multichannel amplitude analyzer (AI-4096) operating in the two-dimensional mode, with the help of which the spectra of recoil protons and of electrons from  $\gamma$  quanta were measured simultaneously. Energy calibration of the neutron spectrometer was carried out with the aid of neutron sources (Po–Be) and monochromatic neutrons from reactions  $d(t, n)\alpha$  and  $\pi^- + p \rightarrow n + \gamma$ . The absolute accuracy of the energy scale for neutrons was  $\pm 5\%$ , and the long-term amplitude instability in the spectrometric channel did not exceed  $\pm 1\%$ . Fig-

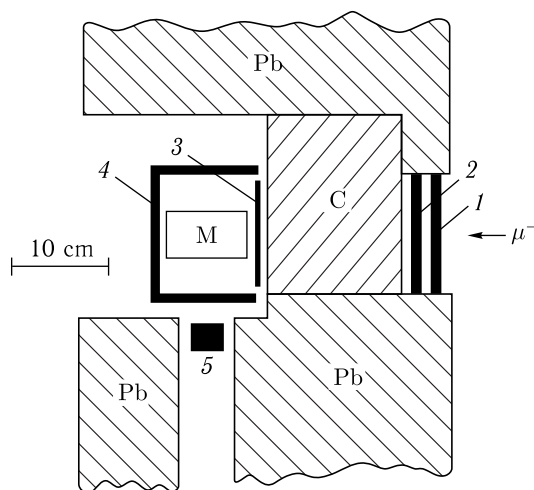


Fig. 13. Arrangement of the hardware in the meson beam [55]

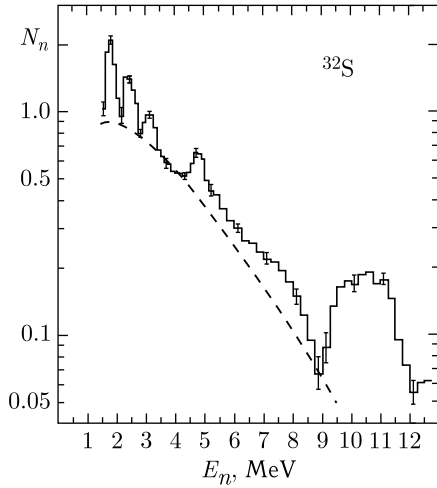


Fig. 14. Energy spectrum of neutrons from the nuclear  $\mu$ -capture reaction in sulfur

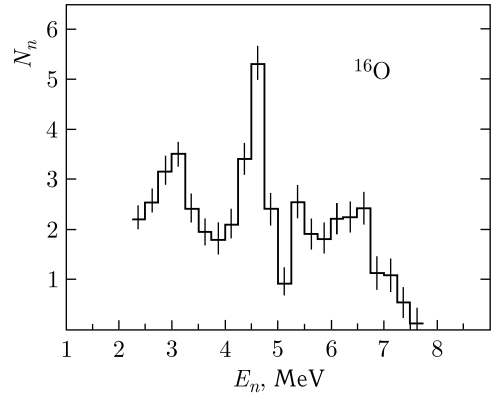


Fig. 15. Energy spectrum of neutrons from the nuclear  $\mu$ -capture reaction in oxygen

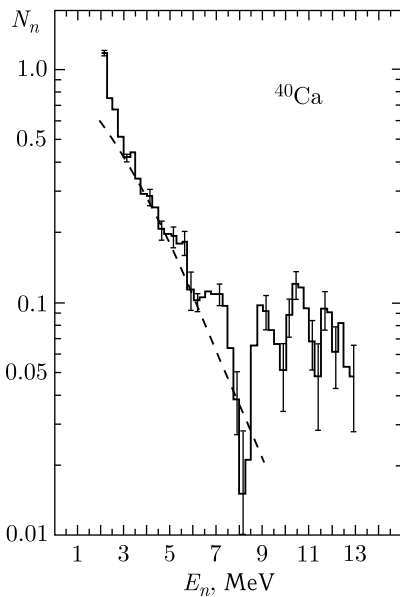


Fig. 16. Energy spectrum of neutrons from  $\mu$ -capture reaction in calcium

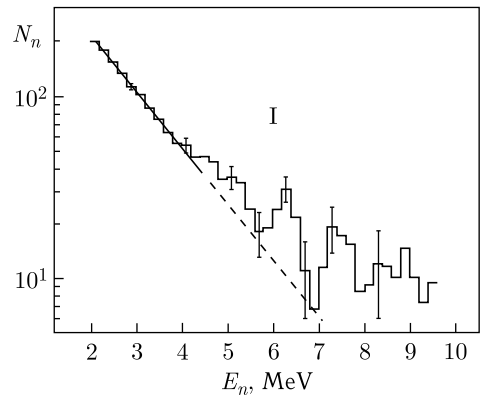


Fig. 17. Energy spectrum of neutrons from the  $\mu$ -capture reaction in iodine

res 14–17 show neutron spectra obtained due to the capture of negative muons by sulfur, oxygen, calcium and iodine nuclei.

As a result of a series of measurements, the following was obtained:

1. The absolute neutron yield (per  $\mu$ -capture act) was measured for  $\mu$  capture in oxygen in the energy range from 2.5 to 7.5 MeV,  $\bar{n} = 0.526 + 0.068$ ; in sulfur, 1.5 to 10 MeV,  $\bar{n} = 0.414 + 0.035$ ; in calcium, 2 to 10 MeV,  $\bar{n} = 0.263 + 0.033$ ; in iodine, 2 to 7. MeV,  $\bar{n} = 0.536 + 0.031$ .

2. The measured neutron spectra show a linear character, which is in agreement with the literature data and with theoretical calculations (dashed lines) [57–59].

Thus, in experiments led by V. S. Evseev, a line structure was found in the neutron spectra emitted during the study of negative muon absorption in the light and intermediate mass atomic nuclei of sulfur, calcium, oxygen and iodine. The validity of the discovery was confirmed by the results obtained by American and Western European physicists.

The discovery was included in the State Register of Discoveries of the USSR under the number 173 in the following wording: “A previously unknown phenomenon of resonance absorption of negative muons by atomic nuclei has been established, consisting in the fact that the absorption of negative muons is a collective excitation of atomic nuclei”.

The priority of the discovery was established by two dates: October 22, 1963 (theoretical substantiation) and October 8, 1968 (experimental confirmation).

## 6. INVESTIGATION OF CHARGED PARTICLE EMISSION IN THE CASE OF NUCLEAR $\mu^-$ CAPTURE

Among the various channels of nucleus splitting in the absorption of muons, the channels with the emission of charged particles occupy a special place. Muon absorption may lead to the excitation of states of the giant resonance type. The decay of these states in some cases leads to the emission of charged particles.

The presence of correlations between nucleons in the nucleus must lead to the emission of charged particles. Of course, in all cases the neutron channel will remain dominant. After the neutron is expelled by the intermediate nucleus  $A - 1$ , thresholds of charged particle escape are often lower than the neutron one in the resulting daughter nucleus  $A - 1$ ,  $Z - 1$ . If the daughter nucleus is formed in a highly excited state, then decay with the emission of a charged particle can well compete with neutron decay. Thus, according to the resonance model [68], the production of a charged particle  $\chi$  in the case of  $\mu$  capture must be related not only to the channel  $(\mu, \nu\chi)$ , but also (and perhaps mainly) to the channel  $(\mu, \nu n\chi)$ . The charged particle spectrum of the resonant capture mechanism should be mostly soft. Its linear structure will appear somewhat less distinct than in the case of neutrons. The characteristics of charged particles in the resonance region are poorly understood.

The first information on the observation of charged particles in the case of the capture of muons by atomic nuclei was obtained long ago, back in experiments with cosmic rays [60]. Experimental data on particle emission, especially at high energies, are very scarce and incomplete [62–64]. The first studies were carried out by Yu. A. Batusov et al. [65] and by H. Morinaga and W. F. Fray in 1953 [66] on heavy photoemulsion nuclei. They showed that the emission of charged particles was sharply suppressed as compared to that of neutrons, amounting to only 3% of the total capture probability. The data on proton and  $\alpha$ -particle emission obtained by the authors could not be simultaneously reconciled with theoretical calculations carried out by C. Ishii [67] based on a statistical model.

A systematic study of the process began later. By now, some experimental and theoretical information has already been accumulated [61], on the basis of which one can systematize the available results and consider the possibilities of their theoretical interpretation.

One effective method of studying the absorption of muons by atomic nuclei with the emission of charged particles is the method of nuclear photoemulsions. Its use made it possible to determine the probability of events with the emission of charged particles and to establish some regularities of this process [65, 68].

A series of measurements on charged particle yields during capture of  $\mu^-$  mesons by nuclei  $^{12}\text{C}$ ,  $^{16}\text{O}$ ,  $^{20}\text{Ne}$ ,  $^{40}\text{Ca}$ ,  $^{80}\text{Br}$  and  $^{108}\text{Ag}$  contained in a photoemulsion were performed at the Laboratory of Nuclear Problems by the group headed by V. M. Sidorov [65]. The integral yield of charged particles from nuclei  $^{12}\text{C}$  and  $^{16}\text{O}$  is about 10%. In nuclei  $^{20}\text{Ne}$  and  $^{40}\text{Ca}$ , the contribution of this channel increases and reaches 15–20%. The emission of charged particles remains almost at the same level in the case of slightly heavier even-even nucleus  $^{58}\text{Ni}$ . However, for odd-numbered nuclei in this region of mass numbers  $A$ , these values already decrease sharply. For Br and Ag nuclei, included in the photoemulsion, the yield of charged particles is 2.9%, for nuclei with mass number  $A > 100$  it does not exceed 1–2%. The maximum yield is for nuclei in the  $^{40}\text{Ca}$  region. The spectrum of the charged particles is predominantly soft. This most likely indicates that the mechanism of charged particle emission is related to secondary processes occurring in the excited intermediate nucleus.

The height of the Coulomb barrier for nuclei with mass number  $A = 60$  reaches 8 MeV, which strongly hinders the escape of slow secondary particles if they are charged. So, naturally, the yield of charged particles as a result of  $\mu$  capture in heavy nuclei is small.

The contribution of the hard component to the total spectrum of charged particles is small and does not exceed 2–3%. The yield of high-energy particles also has a maximum in the region of nuclei with  $Z = 20$ . For a more detailed study of the mechanism of muon capture by nuclei and for a more delicate study of the effect, it is necessary to improve the measuring equipment, increase the efficiency and improve the accuracy of measurements.

For this purpose, a group of physicists of the JINR Laboratory of Nuclear Problems headed by V. G. Zinov conducted a study of  $\mu$ -capture reactions with the emission of charged particles. The aim of this work was to measure energy spectra and the emission probabilities of protons, deuterons and tritium nuclei with energies exceeding 10 MeV in the range of values of the core charge  $10 < Z < 30$ . In order to achieve its objective, the group had to solve the following problems by increasing the luminosity of the entire installation and by enhancing the capabilities of the electronic apparatus:

- a) separation of charged particles by mass;
- b) measurement of the absolute energy spectra of protons, deuterons and tritium nuclei at lowest possible energies;
- c) obtaining the dependence of the yields of these particles on the nucleus charge.

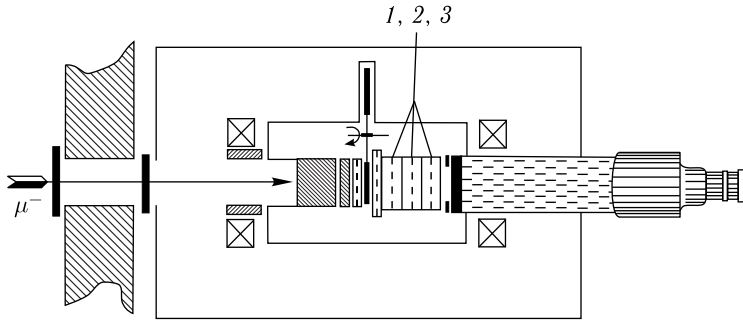


Fig. 18. Block diagram of the setup

Measurements were carried out with nuclei  $^{28}\text{Si}$ ,  $^{32}\text{S}$ ,  $^{40}\text{Ca}$ ,  $^{64}\text{Cu}$ . Figure 18 shows a block diagram of the setup [71].

In the work, negative muons with a momentum of  $130 \text{ MeV}/c$  at the muon tract exit were used. The intensity of the useful part of the time-stretched beam was  $18\text{--}103 \text{ s}^{-1}$ . The energy of emitted charged particles was measured with a spectrometer based on a  $12 \times 2.4 \text{ cm}$  CsI(Tl) crystal. Simultaneous measurement of ionization losses of particles with the help of proportional chambers 1, 2, 3 allowed separating them by mass. Communication of the multidimensional analysis unit on line with the computer ensured accumulation of data, their operative control and further processing.

Tables 5–8 show the final results of measurements and processing of the energy spectra [77].

Table 5. Proton energy spectra (number of particles/capture act  $\times 1 \text{ MeV}$ )  $\cdot 10^4$

$E, \text{ MeV}$	Target			
	C	O	Mg	S
9				$48.4 \pm 1.0$
12	$16.7 \pm 4.0$	$14.7 \pm 2.3$	$21.1 \pm 2.0$	$23.1 \pm 0.8$
15	$9.7 \pm 1.9$	$4.6 \pm 1.8$	$10.5 \pm 1.4$	$21.1 \pm 0.5$
18	$4.4 \pm 1.3$	$6.0 \pm 1.4$	$7.4 \pm 1.0$	$10.3 \pm 0.3$
21	$3.2 \pm 0.9$	$3.2 \pm 1.0$	$4.5 \pm 0.8$	$6.5 \pm 0.2$
24	$2.5 \pm 0.7$	$3.3 \pm 0.7$	$3.5 \pm 0.5$	$4.0 \pm 0.2$
27	$0.8 \pm 0.6$	$0.8 \pm 0.6$	$1.8 \pm 0.4$	$2.6 \pm 0.2$
30	$1.1 \pm 0.6$	$0.9 \pm 0.4$	$1.0 \pm 0.3$	$1.7 \pm 0.1$
33	$0.7 \pm 0.4$	$1.1 \pm 0.3$	$0.8 \pm 0.2$	$1.1 \pm 0.1$
36	$1.0 \pm 0.4$	$0.2 \pm 0.2$	$0.2 \pm 0.2$	$0.74 \pm 0.06$
39	$0.6 \pm 0.4$	$0.1 \pm 0.1$	$0.4 \pm 0.1$	$0.55 \pm 0.05$
42	$0.3 \pm 0.3$	$0.1 \pm 0.1$	$0.13 \pm 0.12$	$0.31 \pm 0.03$
45			$0.19 \pm 0.08$	$0.17 \pm 0.02$
48			$0.10 \pm 0.08$	$0.07 \pm 0.02$
51			$0.10 \pm 0.05$	$0.06 \pm 0.02$
54			$0.04 \pm 0.04$	$0.05 \pm 0.01$
57				$0.02 \pm 0.01$
60				$0.01 \pm 0.01$

Table 6. Deuteron energy spectra (number of particles/capture act  $\times 1 \text{ MeV}$ )  $\cdot 10^4$

$E, \text{ MeV}$	Target			
	C	O	Mg	S
12	$3.7 \pm 2.7$	$9.1 \pm 3.2$	$7.6 \pm 1.9$	$7.8 \pm 0.6$
15	$6.4 \pm 1.8$	$4.4 \pm 2.4$	$7.6 \pm 1.3$	$6.9 \pm 0.5$
18	$5.2 \pm 1.3$	$7.6 \pm 2.0$	$1.6 \pm 1.0$	$4.6 \pm 0.4$
21	$3.5 \pm 0.8$	$3.3 \pm 1.3$	$2.6 \pm 0.7$	$4.0 \pm 0.3$
24	$2.4 \pm 0.7$	$1.8 \pm 0.9$	$0.8 \pm 0.6$	$1.6 \pm 0.2$
27	$0.4 \pm 0.6$	$1.6 \pm 0.6$	$1.4 \pm 0.4$	$1.8 \pm 0.2$
30	$1.5 \pm 0.5$	$0.6 \pm 0.4$	$0.7 \pm 0.3$	$0.7 \pm 0.1$
33	$0.3 \pm 0.4$	$0.3 \pm 0.3$	$0.5 \pm 0.2$	$0.8 \pm 0.1$
36	$0.4 \pm 0.3$	$0.2 \pm 0.3$	$0.2 \pm 0.1$	$0.40 \pm 0.07$
39	$0.4 \pm 0.2$	$0.2 \pm 0.1$	$0.1 \pm 0.1$	$0.33 \pm 0.04$
42				$0.11 \pm 0.03$
45				$0.07 \pm 0.03$
48				$0.07 \pm 0.02$
51				$0.05 \pm 0.02$
54				$0.02 \pm 0.01$

Table 7. Energy spectra of tritons (number of particles/capture act  $\times 1 \text{ MeV}$ )  $\cdot 10^4$

$E, \text{ MeV}$	Target			
	C	O	Mg	S
12	$3.4 \pm 1.6$	$4.0 \pm 2.8$	$4.2 \pm 1.5$	$1.4 \pm 0.3$
15	$1.8 \pm 1.2$	$5.3 \pm 1.7$	$2.9 \pm 1.0$	$0.6 \pm 0.3$
18	$1.4 \pm 1.0$	$2.2 \pm 1.4$	$1.5 \pm 0.6$	$1.2 \pm 0.2$
21	$2.2 \pm 0.8$	$1.5 \pm 0.8$	$0.5 \pm 0.4$	$0.52 \pm 0.15$
24	$1.0 \pm 0.6$	$1.0 \pm 0.5$	$0.2 \pm 0.4$	$0.48 \pm 0.10$
27	$0.3 \pm 0.4$	$0.1 \pm 0.4$	$0.2 \pm 0.3$	$0.19 \pm 0.07$
30	$0.4 \pm 0.3$	$0.1 \pm 0.3$	$0.4 \pm 0.2$	$0.14 \pm 0.05$
33	$0.4 \pm 0.3$	$0.3 \pm 0.3$	$0.0 \pm 0.1$	$0.06 \pm 0.04$
36				$0.05 \pm 0.04$
39				$0.01 \pm 0.04$
42				$0.02 \pm 0.04$
45				$0.01 \pm 0.02$

Figure 19 shows one of the obtained charged particle mass spectra for the  $^{28}\text{Si}$  nucleus. Three peaks are clearly distinguished in the spectrum, corresponding to three tracks of ionization losses of departing particles. A few counts at the edge of the spectrum are interpreted as tritium nuclei. The arrows indicate the positions of the peaks.

The contribution of the resonance mechanism of  $\mu$ -meson capture becomes insignificant at neutron emission energies above 10–15 MeV. In this energy range, the main role can be played by the following two mechanisms: the direct single-nucleon mechanism and the cluster mechanism.

In the first case, the  $\mu^-$  meson interacts with one of the protons of the nucleus and translates it directly into a noncontinuous spectrum [48]. In the second case, the effect is due to short-range nucleon–nucleon correlations. Due

Table 8. **Probabilities of emission of fast protons, deuterons and tritium nuclei in %, per act of capture in nuclei [68]**

Threshold energy, MeV	$^{28}\text{Si}_{14}$			$^{32}\text{S}_{16}$		
	$p$	$d$	$t$	$p$	$d$	$t$
15	$0.88 \pm 0.06$	—	—	$1.15 \pm 0.09$	—	—
18	$0.64 \pm 0.05$	$0.33 \pm 0.03$	—	$0.78 \pm 0.07$	$0.34 \pm 0.04$	—
24	$0.33 \pm 0.03$	$0.15 \pm 0.02$	$0.02 \pm 0.01$	$0.42 \pm 0.05$	$0.17 \pm 0.03$	$0.04 \pm 0.01$
42	$0.04 \pm 0.01$	$0.02 \pm 0.01$	—	$0.06 \pm 0.01$	$0.01 \pm 0.01$	—

Threshold energy, MeV	$^{40}\text{Ca}_{20}$			$^{64}\text{Cu}_{29}$		
	$p$	$d$	$t$	$p$	$d$	$t$
15	$1.30 \pm 0.11$	—	—	$0.60 \pm 0.07$	—	—
18	$0.94 \pm 0.08$	$0.26 \pm 0.04$	—	$0.46 \pm 0.06$	$0.10 \pm 0.03$	—
24	$0.48 \pm 0.06$	$0.19 \pm 0.03$	$0.02 \pm 0.01$	$0.27 \pm 0.05$	$0.08 \pm 0.03$	—
42	$0.06 \pm 0.02$	$0.02 \pm 0.01$	—	$0.04 \pm 0.02$	$0.02 \pm 0.01$	$0.005 \pm 0.005$

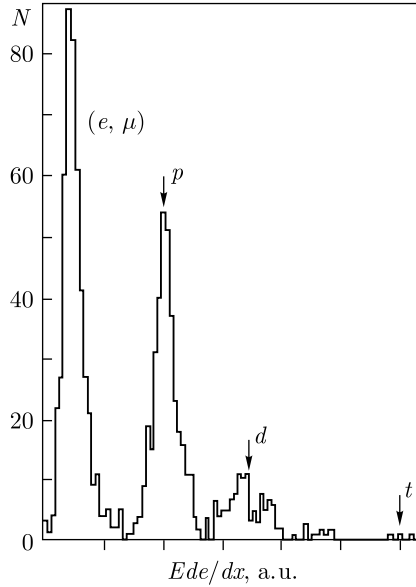


Fig. 19. Charged particle mass spectrum for  $^{28}\text{Si}$ . The arrows indicate the positions of the peaks

to such correlations, subsystems, i.e., clusters of two (quasi-deuteron), four (quasi-alpha particle), etc., nucleons are formed in the nucleus. If the  $\mu$  meson is captured by a proton from such a cluster, the process will no longer be one-nucleon, because the produced neutron will immediately undergo rescattering on the rest of the nucleons of the cluster. Thus, the whole association will take part in the process. The nucleons of the nucleus that are not in the association will not participate directly in this process. The role of the cluster mechanism becomes noticeable in the region beyond the giant resonances as follows from

the analysis of photonuclear reactions. One of the important consequences of this process mechanism is the emission of fast particles. However, even in photonuclear reactions this mechanism is very poorly investigated. As for  $\mu$  capture, it has been estimated in [61] that the quasi-deuteron mechanism can contribute up to 15% to the integral probability of the process.

The authors have analyzed in detail the high-energy part of the spectrum of charged particles for four nuclei, Si, S, Ca and Cu, using a system of semiconductor detectors, which allowed them to separate the particles by charge and mass and to measure their energy [78].

Table 9. Energy spectra of protons and deuterons [78] (see also Fig. 20)

$E$ , MeV	Silicon		Sulfur		Calcium		Copper	
	$N_p$	$N_d$	$N_p$	$N_d$	$N_p$	$N_d$	$N_p$	$N_d$
11	$94 \pm 10$		$83 \pm 10$		$113 \pm 12$		$29 \pm 7$	
14	$134 \pm 12$	$21 \pm 5$	$190 \pm 15$	$7 \pm 4$	$132 \pm 113$	$13 \pm 4$	$53 \pm 9$	$5 \pm 3$
17	$109 \pm 10$	$36 \pm 6$	$128 \pm 12$	$36 \pm 7$	$95 \pm 11$	$20 \pm 5$	$30 \pm 7$	$7 \pm 3$
20	$89 \pm 9$	$47 \pm 7$	$65 \pm 9$	$24 \pm 6$	$68 \pm 9$	$6 \pm 4$	$28 \pm 6$	$1 \pm 3$
23	$50 \pm 7$	$33 \pm 6$	$60 \pm 8$	$35 \pm 7$	$52 \pm 8$	$12 \pm 5$	$9 \pm 4$	$2 \pm 3$
26	$47 \pm 7$	$18 \pm 4$	$44 \pm 7$	$13 \pm 4$	$37 \pm 7$	$12 \pm 4$	$17 \pm 5$	$5 \pm 3$
29	$27 \pm 5$	$10 \pm 3$	$31 \pm 6$	$13 \pm 4$	$27 \pm 6$	$11 \pm 4$	$6 \pm 3$	$3 \pm 2$
32	$21 \pm 5$	$11 \pm 3$	$19 \pm 5$	$8 \pm 3$	$17 \pm 5$	$3 \pm 2$	$9 \pm 3$	$4 \pm 2$
35	$15 \pm 4$	$12 \pm 4$	$16 \pm 4$	$7 \pm 3$	$14 \pm 4$	$4 \pm 4$	$5 \pm 3$	$1 \pm 2$
38	$12 \pm 4$	$7 \pm 3$	$8 \pm 3$	$7 \pm 3$	$11 \pm 4$	$7 \pm 3$	$11 \pm 3$	
41	$12 \pm 4$	$5 \pm 2$	$8 \pm 3$	$7 \pm 3$	$5 \pm 3$	$1 \pm 4$	$2 \pm 2$	
44	$6 \pm 2$	$2 \pm 1$	$4 \pm 2$	$3 \pm 2$	$5 \pm 3$	$3 \pm 2$	$1 \pm 1$	$2 \pm 1$
47	$1 \pm 1$	$2 \pm 1$	$6 \pm 3$	$2 \pm 1$	$2 \pm 1$		$4 \pm 2$	$1 \pm 1$
50	$7 \pm 3$	$4 \pm 2$	$1 \pm 1$		$4 \pm 2$		$1 \pm 1$	
53		$1 \pm 1$	$4 \pm 2$		$3 \pm 2$	$1 \pm 1$	$1 \pm 1$	
56			$2 \pm 1$		$1 \pm 1$	$1 \pm 1$	$1 \pm 1$	$1 \pm 1$

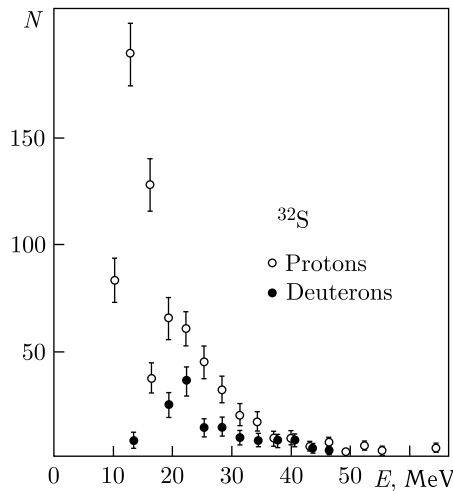


Fig. 20. Energy spectrum of protons and deuterons in  $^{32}\text{S}$  nucleus muon capture [68]

From the experimental data presented in Table 9, it follows that the fraction of high-energy charged particles is quite large. Table 9 and Fig. 20 show the integral yield of high-energy protons and deuterons in the case of  $\mu$ -meson capture by some light nuclei [78].

Thus, the following conclusions are drawn as a result of the research [68]:

1. The greater the mass of a charged particle, the lower is the probability of its emission.
2. In the spectra there are practically only protons and deuterons.
3. With increasing charge  $Z$  of the target nucleus, the share of deuterons in the total yield of charged particles drops.
4. The proton yield has a maximum in the region of calcium,  $Z = 20$ .
5. Energy spectra of charged particles extend up to 50–60 MeV and are characterized by a smooth exponential dependence (Fig. 18).
6. Within the limits of measurement errors, proton spectra from S and Ca nuclei agree with the neutron spectra measured in [69], but quite strongly differ from the spectra given in [57, 70].

## 7. SEARCH FOR A THIRD TYPE OF MUON CAPTURE BY THE NUCLEUS

All of the above processes occur within the two well-known types of excitation of the nucleus in muon atoms: excitation in the process of muon cascade transitions (resonant or radiationless) and excitation as a result of  $\mu$  capture by the nucleus. As mentioned above, the search for the first type of excitation led to the theoretical and then to the experimental discovery of the process, for which it was included in the All-Union Register of Discoveries of the USSR [10]. The third possible fate of the muon, which fell into the sphere of influence of the nucleus, remained without attention of all “muonists”, although indirectly, as if in passing, the possibility of the muon decaying on the  $K$  orbit of the nucleus was mentioned, but without a consideration of the process continuing to occur in the nucleus. An experiment to find this process was imminent. The idea of the experiment was to theoretically and experimentally investigate the possibility of a third type of excitation of the nucleus in the case of a bound muon decaying. The physics of this excitation is similar to the well-known shaking of electron shells in nuclear  $\beta$  decay, when the charge of the nucleus changes by one. The energy released in  $\mu$  decay is much higher than the energy of low-lying nuclear excitations. The potential acting from the bound muon on the nucleus is almost instantly “turned off”, which causes quantum transitions in the latter. Since the muon with orbital momentum  $\ell = 0$  creates a spherically symmetric electromagnetic field around the nucleus, its instantaneous removal causes electromagnetic shaking of the nucleus, and this explains the process by which predominantly monopole excitation of the nucleus must occur. The study of the excitation of the nucleus during the decay of a bound muon, which is of independent interest — the discovery of a new process and verification of the correctness of our ideas about it, could provide in the future a new additional method to study the nuclear monopole states [72]. The muon, in passing through

three stages of the process of mesoatom formation, reaches the  $K$  orbit in a time of  $10^{-10}$ – $10^{-14}$  s. Its fate ends either by nuclear capture or decay according to the scheme  $\mu^- \rightarrow e^- + 2\nu$ . As shown in the theoretical works of I. S. Batkin [73], the low-lying monopole states of the nucleus can be excited during the decay of a bound  $\mu^-$  meson in the mesoatom. This process also seems to be a unique tool to investigate monopole states of atomic nuclei. But the main goal of the experiment is to detect monopole excitation of the nucleus, which would serve as evidence for the existence of a third type of  $\mu$ -capture excitation of the nucleus. The first estimates of this process based on the Davydov–Chaban droplet model yielded a probability  $w \sim 1.6 \cdot 10^{-2}$  [73]. The following estimate, made by I. A. Mitropolsky, is based on the microscopic approach which considers the excitation of several  $0^+$  states and gives a much lower probability of excitation of the lowest  $0^+$  level:  $w \leq 3 \cdot 10^{-4}$  [74]. When planning the experiment, one should bear in mind that the nuclear transition can be converted. The main purpose of the experiment is to register  $\gamma$  quanta in coincidence with the decay electron. This experiment was proposed in 1976 by the author of this review to Academician B. Pontecorvo, the discoverer of radiationless muon capture. The proposal was accepted and strongly supported.

A  $^{152}\text{Sm}$  nucleus (Fig. 21) was chosen as the object of study.

In Table 10, probabilities of conversion and radiation discharge of  $0^+$  levels in deformed nuclei are given. The nucleus  $^{232}\text{U}$  is given for comparison, the first  $0^+$  level of which has a close energy [74].

From the table, one can see that the first  $0^+$  level in  $^{152}\text{Sm}$  will be discharged mainly by  $\gamma$  quanta, while the  $0^+$  level in  $^{232}\text{U}$  with the same energy will be almost completely converted.

In 1976, the LNP accelerator was stopped for an upgrade. It was necessary to reorient to the accelerator of Leningrad Institute of Nuclear Physics (LINP)

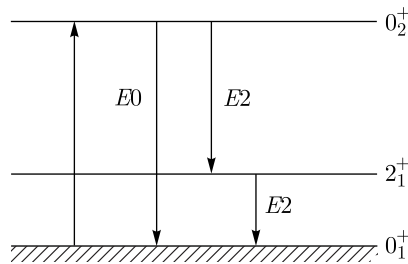


Fig. 21. Scheme of the excitation and decay of the nuclear  $0^+$  level of a  $^{152}\text{Sm}$  nucleus [75]

Table 10. **Probabilities of conversion and radiation discharge of  $0^+$  levels in deformed nuclei [74]**

Nucleus	$E_{0^+}$ , MeV	$E_{2^+}$ , MeV	$X$	$T_e(E2)/T_\gamma(E2)$	$T_e(E0)/T_\gamma(E2)$
$^{152}\text{Sm}$	0.685	0.122	0.07	0.01	0.02
$^{232}\text{U}$	0.695	0.048	0.17	0.02	0.96
<i>Note.</i> $X = B(E0; 0_1^+ - 0_0^+)/B(E2; 0_1^+ - 2_0^+)$ .					

in Gatchina. The Scientific Council of the LINP accepted the proposal of the experiment. The experimental setup MEGA (MEsonGAMma), consisting of a system of scintillation counters 1, 2, 3, 4 to provide for muon stopping in the target, a Ge(Li)  $\gamma$  detector with a sensitive volume of 55 cm<sup>3</sup> and a Cherenkov counter of electrons 5a + 5b made of heavy lead glass TF-1, was mounted on the LINP muon beam. The muon beam provided  $\sim 10^4$  s<sup>-1</sup> stops in a 117 g target. The target was in the form of samarium trioxide powder Sm<sub>2</sub>O<sub>3</sub> enriched up to 98% <sup>152</sup>Sm. A scheme of the MEGA experimental setup designed to study the excitation of nuclei during bound muon decay is shown in Fig. 22.

The registration of  $\gamma$  quanta is carried out using a Ge(Li) detector of large volume. Particular requirements are imposed on the timing characteristics of the setup which determine the efficiency of useful signal extraction. Figure 23 shows a time spectrum obtained with the MEGA experimental facility. The time windows marked with numbers correspond to the following processes: 1 – background radiation in “negative” time before muon stopping, 2 – prompt spectrum of muonic X-ray radiation, 3 – delayed  $\gamma$  quanta from nucleus after capture or decay of muon, 4 – background spectrum.

The working region is the third time window, the exponential decay of the radiation intensity in which is determined by the lifetime of the muon in the *K* orbit of the mesoatom. From measurements at MEGA, this time for <sup>152</sup>Sm is  $\sim 85$  ns, and the width of the Gaussian distribution of muonic X rays (window 2) is less than 5 ns.

During preliminary experimental sessions,  $1.5 \cdot 10^9$  muon stops in a target were recorded [75–76].

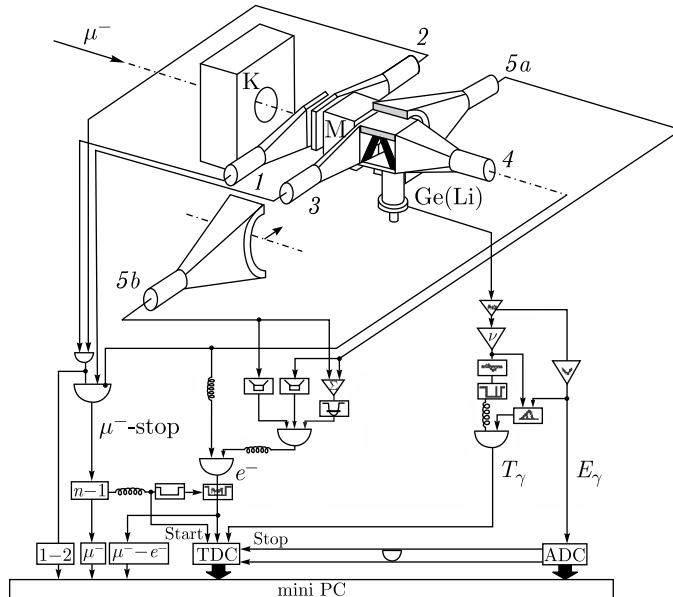


Fig. 22. Block diagram of the MEGA pilot plant

Figure 24 shows the spectrum of delayed gamma rays from nuclear transitions caused by muon decay in the  $K$  orbit of the mesoatom, coinciding with the fast electron [76]. The arrow indicates the place where the peak from the sought transition should be. The dark area on the energy scale corresponds to the width of the peak at half-height; the shaded area, to that at 0.1 height.

The experimental data allow us to establish an upper limit for the probability of excitation of the first  $0^+$  level of  $^{152}\text{Sm}$  in the decay of a bound muon:  $w < 5 \cdot 10^{-3}$ . This does not allow us to confirm the correctness of the theoretical results given in Ref. [74], but it experimentally closes the early estimate of the probability  $w \sim 1.6 \cdot 10^{-2}$  [73]. The results give us hope for a successful development of research in this direction [76]. Obviously, this experiment should be repeated with much improved apparatus so that high-statistics measurements can be made in very low background conditions.

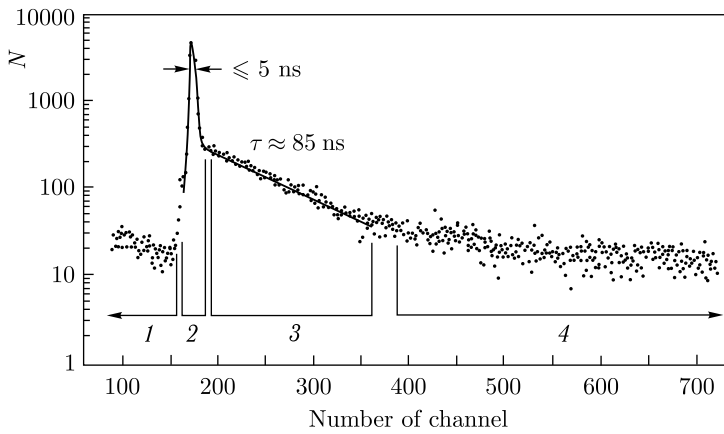


Fig. 23. Timing spectrum of  $\gamma$  radiation during muon stopping in a  $^{152}\text{Sm}$  target. One channel is 1 ns

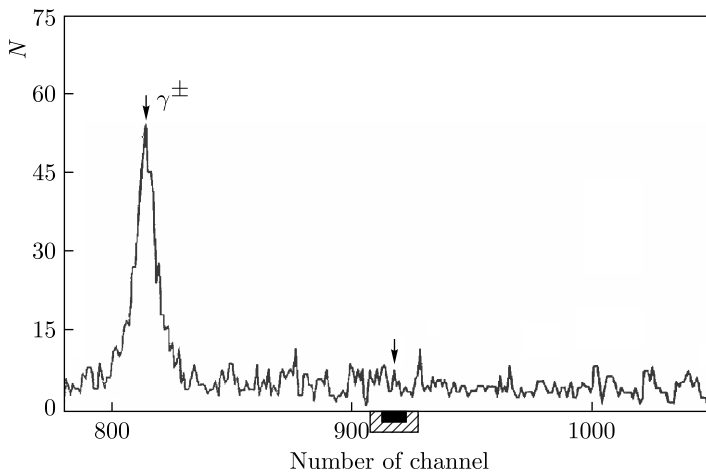


Fig. 24. Spectrum of delayed  $\gamma$  quanta with selection on the basis of the presence of fast electron from muon decay

## CONCLUSIONS

In summary, the results of completely different and independent experimental approaches to the problem of interaction of muons with nuclei have been described. The experimental data require refinement, in particular, with respect to fission fragment spectroscopy, secondary particle spectroscopy, and statistical accuracy. All of the experimental methods described rely on interpretation within theoretical models. Improvements in each of these parts will mutually stimulate refinements or new paths in subsequent studies.

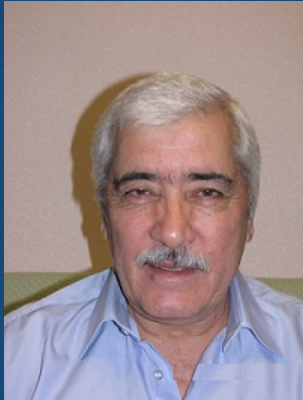
**Acknowledgements.** The author would like to thank V. V. Glagolev for his interest and stimulating suggestion to write this review, and I. A. Mitropolsky for reading the review and making very useful comments and corrections. The author is also grateful to G. Pontecorvo, whose help in editing the English version of the article was decisive, and to E. Velitcheva for preparing the computer design of the text.

## REFERENCES

1. Kirillov-Ugryumov V. G., Nikitin Yu. P., Sergeev F. M. *Atoms and Mesons*. Moscow: Atomizdat, 1980.
2. Balashov V. V., Korenman G. Ya., Eramzhyan R. A. *Absorption of Mesons by Atomic Nuclei*. Moscow: Atomizdat, 1978.
3. Charalambus S. // *Nucl. Phys. A*. 1971. V. 166. P. 145–161.
4. Wheeler J. A. // *Rev. Mod. Phys.* 1949. V. 21. P. 133.
5. Zaretsky D. F. // *Proc. of the Second Intern. Conf. on the Peaceful Uses of Atomic Energy*. Geneva, 1958.
6. Belovitsky G. E., Kashukeyev N. T., Mihul A., Petrashku M. G., Romanova T. A., Tikhomirov F. A. *JINR Preprint*. Dubna, 1959.
7. Mihul A. K., Petrashku M. G. // *Dokl. Akad. Nauk SSSR*. 1959. V. 124, No. 1. P. 66.
8. Petrashku M. G., Mihul A. K. // *Dokl. Akad. Nauk SSSR*. 1959. V. 126, No. 4. P. 752.
9. Diaz J. A., Kaplan S. N., MacDonald B., Pyle R. V. // *Phys. Rev. Lett.* 1959. V. 3. P. 234.
10. Balatz M. Y., Kondratyev L. N., Landsberg L. G., Lebedev P. I., Obukhov Y. V., Pontecorvo B. // *Zh. Eksp. Teor. Fiz.* 1960. V. 38, No. 6. P. 1715.
11. Karpeshin F. F., Listengarten M. A., Band I. M., Sliv L. A. // *Izv. Akad. Nauk SSSR, Ser. Fiz.* 1976. V. 40. P. 1164.
12. Barit I. Y., Belovitsky G. E., Zaretsky D. F. *Preprint of IN RAS USSR P-0058*. Moscow, 1977.
13. Demkov Yu. N., Zaretsky D. F., Karpeshin F. F., Listengarten M. A., Ostrovsky V. N. // *Pis'ma Zh. Eksp. Teor. Fiz.* 1978. V. 28, No. 5. P. 287.
14. Demkov J. N. // 1963. *JETP*. V. 45. P. 195.
15. Zaretsky D. F., Karpeshin F. F. *Preprint of LINP of the USSR Academy of Sciences*. Leningrad, 1977.
16. Cojocaru V., Marinescu L., Petrascu M., Voiculescu G., Ignatenko A., Omelianenko M. // *Phys. Lett.* 1966. V. 20, No. 1. P. 53.

17. Viola V. // Nucl. Data. 1976. V. 1. P. 391.
18. Zaretsky D. F., Karpeshin F. F. // Yad. Fiz. 1979. V. 29, No. 2. P. 306.
19. Pelle R. W., Meienshein F. S. // Phys. Rev. C. 1971. V. 3. P. 373.
20. Rösel C., Karpeshin F. F., David P., Hänscheid H., Konijn J., de Laat C. T. A. M., Paganetti H., Risse F., Sabirov B., Schaller L. A., Schellenberg L., Schrieder W., Taal A. // Z. Phys. A. 1993. V. 345. P. 425–426.
21. Karpeshin F. F. // Izv. Akad. Nauk SSSR. 1983. V. 47. P. 18; Bull. Acad. Sci. USSR, Ser. Fiz. 1983. V. 47. P. 183.
22. de Laat C. T. A. M. Rijksuniversiteit Utrecht, Report FI 91-1. 1991
23. Hänscheid H., David P., Folger H., Konijn J., de Laat C. T. A. M., Petitjean C., Reist H. W., Risse F., Rösel C., Schaller L. A., Schellenberg L., Schrieder W., Simons L. M., Taal A. // Z. Phys. A. 1992. V. 342. P. 111–120.
24. Chultem D., Cojocar V., Ganzorig Dz., Kim Si Chwan, Krogulski T., Kuznetsov V. D., Ortlepp H. G., Polikanov S. M., Sabirov B. M., Schmidt U., Wagner W. // Nucl. Phys. A. 1975. V. 247. P. 452; Chultem D. et al. JINR, E15-8134. Dubna, 1974.
25. Aleksandrov B. M., Buklanov G. V., Fromm W. D., Ganzorig Dz., Krivokhatki A. S., Krogulski T., Polikanov S. M., Sabirov B. M. JINR, E15-8628. Dubna, 1975.
26. Ganzorig Dz., Krogulski T., Kuznetsov V. D., Polikanov S. M., Sabirov B. M. JINR, E15-9365. Dubna, 1975.
27. Buttsev V. S., Ganzorig J., Kojokaru V., Krogulski T., Ortlepp H. G., Polikanov S. M., Sabirov B. M., Fromm W. D., Schmidt U., Chulthem D. // Pis'ma Zh. Eksp. Teor. Fiz. 1976. V. 23, No. 9. P. 534.
28. Kaplan S. N. et al. // Phys. Rev. 1958. V. 112. P. 968.
29. Sens J. C. // Phys. Rev. 1959. V. 113. P. 679.
30. Diaz J. A. et al. // Nucl. Phys. 1963. V. 40. P. 54.
31. Budick B. et al. // Phys. Rev. Lett. 1970. V. 24. P. 604.
32. Meyers W. D., Swiatecki W. J. Univ. California Rep. UCRL-11980.
33. Backe H. // Z. Phys. 1971. V. 241. P. 435.
34. Routti J. T. Report UCRL-19452.
35. Hüfner J. H. // Z. Phys. 1966. V. 195. P. 365.
36. Akimov Yu. K. et al. // Nucl. Instr. Meth. 1972. V. 104. P. 581.
37. David P., Rösel C., Karpeshin F. F., Sabirov B. Recent Facets of Nuclear Fission Dynamics and Properties of Heavy Muonic Atoms. Invited talk presented at the Workshop on Muonic Atoms and Molecules, Monte Verita, Ascona, Apr. 5–9, 1992.
38. Polikanov S. Meson, Hyperon, and Antiproton Induced Fission // Nucl. Phys. A. 1989. V. 502. P. 195.
39. Ganzorig Dz. et al. // Phys. Lett. B. 1978. V. 78. P. 41; Nucl. Phys. A. 1980. V. 350. P. 276.
40. Berti W. et al. (SINDRUM). SIN-Proposal R-80-06.2. 1981.
41. Metag V. et al. // Nucl. Instr. Meth. 1974. V. 114. P. 445.
42. Condo G. T. et al. // Phys. Rev. C. 1984. V. 29. P. 1531.
43. Il'inov A. S. et al. // Nucl. Phys. A. 1982. V. 38. P. 378.
44. Pontecorvo B. // Phys. Rev. 1950. V. 72. P. 246.
45. Hildebrand R. // Phys. Rev. Lett. 1962. V. 8. P. 34.
46. Weisenberg A. O. Mu Meson. Moscow: Nauka, 1964.
47. Balashov V. V., Beljaev V. B., Eramzhyan R. A., Kabachnik N. M. // Phys. Rev. 1964. V. 9. P. 168; JINR Preprint P2-3258. Dubna, 1967.

48. *Eramzhyan R. A.* // IV Intern. Conf. on High Energy Physics and Structure of Nuclei, Dubna, 1971. P. 449.
49. *Evseyev V. S.* // Ibid. P. 475.
50. *Balashov V. V.* // Ibid. P. 167.
51. *Balashov V. V., Eramzhyan R. A.* // Atom. Energy Rev. 1967. V. 5, No. 3. P. 3.
52. *Evseev V. S., Kozlowski T., Roganov V., Woitkowska J.* // Phys. Lett. B. 1969. V. 28. P. 553.
53. *Wojtkowska J., Evseev V. S. et al.* // Yad. Fiz. 1972. V. 15. P. 1154.
54. *Evseev V. S.* // Intern. Conf. on High Energy Physics and Structure of the Nucleus. Dubna, 1971.
55. *Wojtkowska J., Evseev V. S., Kozlowski T., Roganov V. S.* JINR Preprint R13-6053. Dubna, 1971.
56. *Kozlowski T.* // Nukleonika. 1968. V. XIII. P. 999.
57. *Evseyev V., Kozlowski T., Roganov V., Wojtkowska J.* // Phys. Lett. 1969. V. 228. P. 553; Proc. of the III Conf. on High Energy Phys. and Nucl. Structure. New York; London: Plenum Press, 1970. P. 157.
58. *Krieger M. H.* Ph.D. Thesis. Columbia Univ., 1989.
59. *Pratt T. A. E. C.* // Nuovo Cim. B. 1969. V. 61, No. 1. P. 119.
60. *George E. P., Evans J.* // Proc. Phys. Soc. A. 1951. V. 64. P. 193.
61. *Singer P.* // Springer Tracts Mod. Phys. 1974. V. 71. P. 39;  
*Uberal H.* // Ibid. P. 1.
62. *Fray W. F.* // Phys. Rev. 1952. V. 85. P. 676.
63. *Kotelchuk D.* // Nuovo Cim. 1964. V. 34. P. 27.
64. *Weisenberg A. O. et al.* // Yad. Fiz. 1975. V. 21. P. 652.
65. *Batusov Yu. A. et al.* // Ibid. P. 1215.
66. *Morinaga H., Fray W. F.* // Nuovo Cim. 1953. V. 10. P. 308.
67. *Ishii C.* // Prog. Theor. Phys. 1959. V. 21. P. 663.
68. *Batusov Yu. A., Eramzhian R. A.* // Fiz. Elem. Chastits At. Yadra. 1977. V. 8, No. 2. P. 229.
69. *Sundelin R. M.* // Phys. Rev. Lett. 1968. V. 20. P. 1198.
70. *Krieger M.* Preprint Columbia Univ. NEVIS-172. 1969.
71. *Balandin M. P., Grebenyuk V. M., Zinov V. G., Kozlowski T., Konin A. D.* JINR, P13-10874. Dubna, 1977.
72. *Voinova-Eliseyeva N. A., Mitropolsky I. A.* // Fiz. Elem. Chastits At. Yadra. 1986. V. 17. P. 1173.
73. *Batkin I. S.* // Yad. Fiz. 1976. V. 24. P. 254; 1978. V. 38. P. 1449.
74. *Mitropolsky I. A.* LINP, No. 680. Leningrad, 1981.
75. *Abazov V. M., Voinova-Eliseeva N. A., Gordeev V. A., Kutuzov S. A., Mitropolsky I. A., Ortlepp H.-G., Sabirov B. M., Soliakin G. E.* // Izv. Akad. Nauk SSSR, Fiz. Ser. 1988. V. 52, No. 5. P. 1008.
76. *Sabirov B. M., Abazov V. M., Kutuzov S. A., Solyakin G. E.* Nuclear Gamma Radiation Caused by a Muon at Rest in  $^{152}\text{Sm}$  // Phys. Part. Nucl. 2020. V. 51, No. 6. P. 1304.
77. *Balandin M. P., Grebenyuk V. M., Zinov V. G., Kozlovsky T., Konin A. D.* JINR, R15-11215. Dubna, 1978.
78. *Budyashov Yu. G., Zinov V. G., Konin A. D., Mukhin A. I., Chatrchyan A. M.* // Zh. Eksp. Teor. Fiz. 1971. V. 60, No. 1. P. 19.
79. *Sabirov B. et al.* Nuclear Processes Induced by Muon Decay at the  $K$ -Orbit of Muonic Atom. JINR Commun. E15-2012-61. Dubna, 2012.



Basar Mukhitdinovich SABIROV graduated in 1967 from the Faculty of Physics of Tashkent State University with specialization "Nuclear Physicist". Since 1969 he has been an employee of the JINR Laboratory of Nuclear Problems. He gained experience in working with muonic atoms to study nuclear, atomic and chemical properties of matter, actively participated in experiments on the use of muonic atoms in medical and biological space research together with the Institute of Medical and Biological Problems of RAS. B. M. Sabirov is the author and participant of the experiment on investigation of monopole excitation of nuclei at decay of bound muon. He participated in the creation of the muon system in the D0 experiment at Fermilab (USA) where he acted as the head of the JINR group. He carried out extensive research work on modernization of the cryomodule of the International Linear Collider (ILC) and received a Patent for invention. Currently he is engaged in the production and research of straw tubes for the international COMET experiment in Japan.